(NASA-CR-161676) WIND PROFILES FOR SPACE SHUTTLE LOADS ANALYSIS Final Report (Science Applications, Inc., Huntsville, Ala.) 75 p HC A04/MF A01 CSCL 04B G3/47

N81-20666

Unclas 41769

FINAL REPORT

WIND PROFILES FOR SPACE SHUTTLE LOADS ANALYSIS

CONTRACT NAS8-32839

SCIENCE APPLICATIONS INCORPORATED

SAI-79-819-HU

FINAL REPORT

WIND PROFILES FOR SPACE SHUTTLE LOADS ANALYSIS

CONTRACT NAS8-32839

29 DECEMBER 1978

PREPARED BY:

STANLEY I. ADELFANG

FOR:

NATIONAL AERONAUTICS AND SPACE ADMINISTRATION
GEORGE C. MARSHALL SPACE FLIGHT CENTER
MARSHALL SPACE FLIGHT CENTER, ALABAMA 35812

SCIENCE APPLICATIONS, INC.

2109 W. CLINTON AVENUE, SUITE 800
HUNTSVILLE, ALABAMA 35805 (205) 533-5900

FOREWORD

This study was conducted under NASA Contract NAS8-32839 with Marshall Space Flight Center, Atmospheric Sciences Division, Space Sciences Laboratory. Mr. Orvel E. Smith was the technical monitor and Mr. Edward M. Harper was the Contracting Officer.

TABLE OF CONTENTS

LIST OF ILLUSTRATIONS

LIST OF ILLUSTRATIONS (Cont'd)

LIST OF ILLUSTRATIONS (Cont'd)

LIST OF TABLES

LIST OF TABLES (Cont'd)

I. INTRODUCTION

This report describes an anlaysis of the small scale wind velocity perturbations in vertical wind profiles at Cape Kennedy, Florida. The overall objective of the analysis is the derivation of new information that is useful for simulations of Space Shuttle ascent thru the perturbed atmosphere. Previous representations of wind velocity perturbations include power spectra (Ref. 1, 2, 3), exceedance statistics (Ref. 3) and idealized singularities and quasi-sinusoidal wave patterns (Ref. 2). Each of these representations by themselves is an important aspect of perturbation profiles. Power spectra are suitable for representation of the random component of the perturbations. Perturbations having a known power spectrum are simulated by application of an appropriate filter to a noise generator. These simulated perturbations do not contain the singularities and quasi-sinusonidal variations that are observed in wind profiles. Prior to this study, the available statistical data did not permit specification of various aspects of idealized singularities and wavelike perturbations with a reasonable degree of confidence. The information developed as a result of the analysis described in Section III of this report is suitable for the further development of idealized models.

The term perturbation is used here instead of the more common term, gust. According to the conventional approach, a gust profile is calculated by applying a high-pass digital filter to a Jimsphere profile; all the speeds in the filtered profile are defined as gusts. In this study the high-pass filtered profile is defined as a residual profile and the maximum residual in the vicinity of a specified reference height is defined as the gust. Gusts defined in this manner represent the perturbation peaks. A detailed discussion of the calculation of residual profiles and gusts is given in Section II. The meteorological coordinate system, the data sample and Jimsphere profiles are also described in Section II. Recommendations and conclusions are presented in Section IV.

II. TECHNICAL BACKGROUND

A. Meteorological Coordinate System.

The basic winds aloft data are recorded in terms of wind direction, θ and magnitude, W. The wind vector is expressed in the standard meteorological coordinate system in which the direction from which the wind is blowing is measured in degrees clockwise from true north. The zonal component, u, of the wind vector is positive for a west (west to east) wind ($\theta=270^o$) and negative for an east (east to west) wind ($\theta=90^o$); the meridional component, v, is positive for a south (south to north) wind ($\theta=180^o$) and negative for a north (north to south) wind ($\theta=0^o$). The components are calculated from θ and W according to:

$$u = -W \sin \theta, \qquad 0 \leq \theta \leq 360^0 \tag{1}$$

$$v = -W \cos \theta, \tag{2}$$

The relation between θ defined above and the angle defined in standard mathematical polar form is:

$$\theta = 270 - \theta_{Math} \tag{3}$$

B. Data Sample.

The data consist of 1800 Jimsphere profiles (150 per month) from Cape Kennedy, Florida (Ref. 4). The data were obtained under a Space Shuttle Level II directive that specifies the demonstration of vehicle design validity using 150 Jimsphere wind profiles representative of each month. Two months (April, February) were chosen for analysis in this study. April data were used to develop and refine the analysis procedure which could be applied efficiently to other months when required. April was also of interest because it coincided with the planned[1] Orbital Flight Test Mission. The February data were chosen because they are representative of the winter season at Cape Kennedy. The number of soundings for each month for each year of the sampling period is illustrated in Figure 1.

C. Jimsphere Data.

Jimsphere wind profile data are obtained by precision radar (FPS-16) tracking of an ascending (4-5 m/s) 2-meter diameter superpressure balloon with a roughened surface. The balloon positions, determined every 0.1 second, are smoothed to provide mean positions at each 25-meter interval of ascent (Ref. 3). Differences in position between

[1] Rescheduled

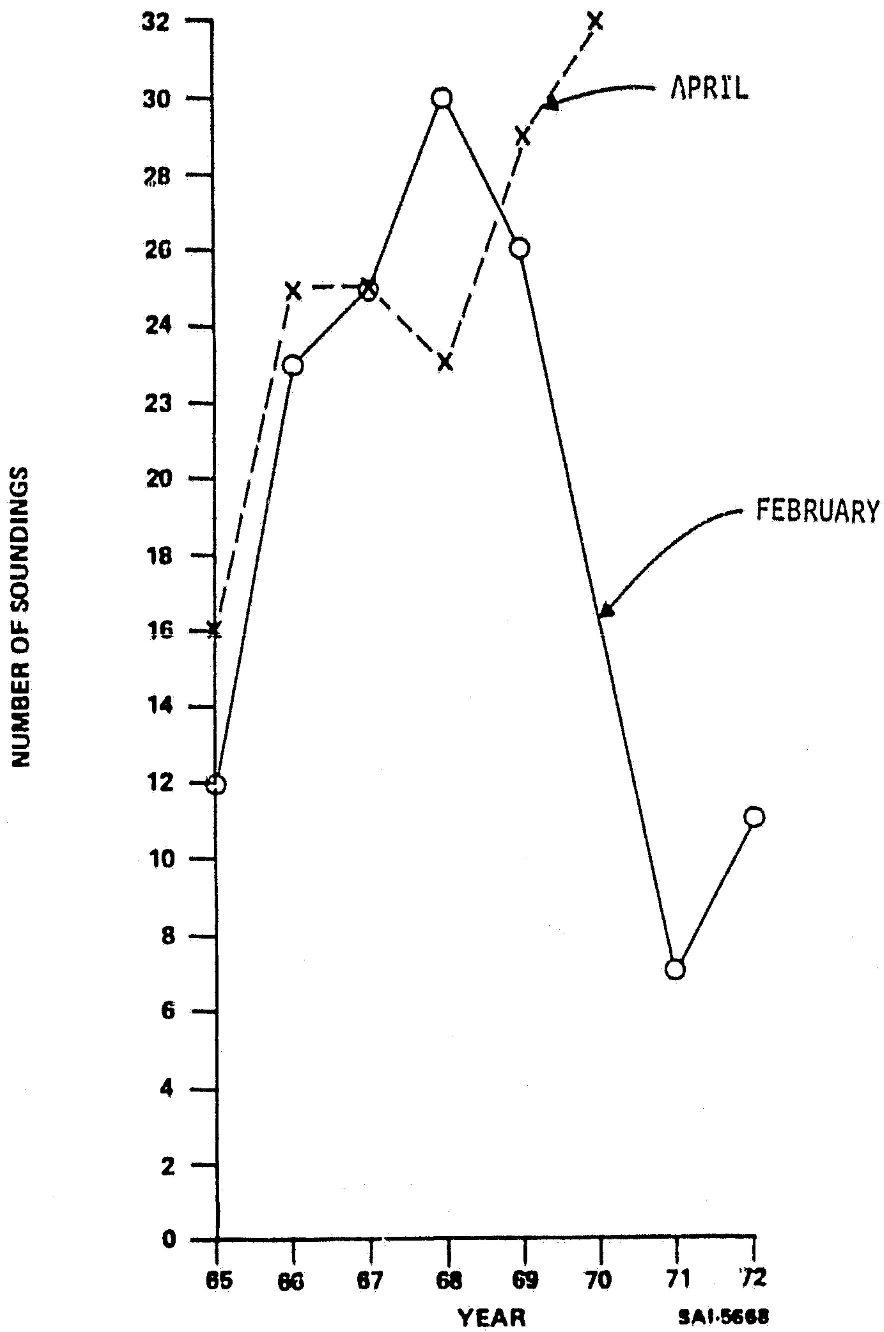

Figure 1. Distribution of February and April Jimsphere Soundings

alternate 25-meter levels then indicate the mean wind for the corresponding 50-meter layer, and are reported as the wind at the 25-meter level in the middle of the 50-meter layer. Thus, the basic data analyzed here are wind speeds and directions for 50-meter layers, overlapping by 25 meters. Even when the overlaps are eliminated, winds for successive 50-meter layers are not independent, because they are based on the smoothed balloon position at the common boundary. Only when at least 25 meters intervenes between two layers (i.e., winds reported for levels at least 75 meters apart) can two winds be considered independent observations (Ref. 3).

Expressions for the amplitude response, $G(\lambda)$, of the Jimsphere system to wind perturbation wavelengths that are small relative to the length of the wind profile have been derived by Luers and Engler (Ref. 5),

$$G(\lambda) = \frac{\cos\left(\frac{\pi S}{3\lambda}\right) \sin^2\left(\frac{\pi S}{3\lambda}\right)}{\left(\frac{\pi S}{3\lambda}\right)^2} \tag{4a}$$

and by DeMandel and Krivo (Ref. 6).

$$G(\lambda) = \frac{\sin\left(\frac{4\pi w}{\lambda}\right) \sin\left(\frac{50\pi}{\lambda}\right)}{200w\left(\frac{\pi}{\lambda}\right)^2} \tag{4b}$$

where, S = smoothing interval = 75m
λ = wavelength(m)
w = Jimsphere balloon ascent rate

The amplitude response is equivalent to the ratio $A(\lambda)/A^*(\lambda)$; where $A^*(\lambda)$ is the true amplitude and $A(\lambda)$ is the amplitude measured with the Jimsphere system. As illustrated in Figure 2, the Jimsphere system does not measure wavelengths less than 50m; for λ=90m the measured amplitude is one-half the true amplitude.

The Jimsphere data represent an order of magnitude improvement in resolution when compared to conventional Rawinsonde wind profiles. The perturbations observable with the Jimsphere system permit a more realistic assessment of the structural response of spacecraft and launch vehicles to small scale wind gust and shear.

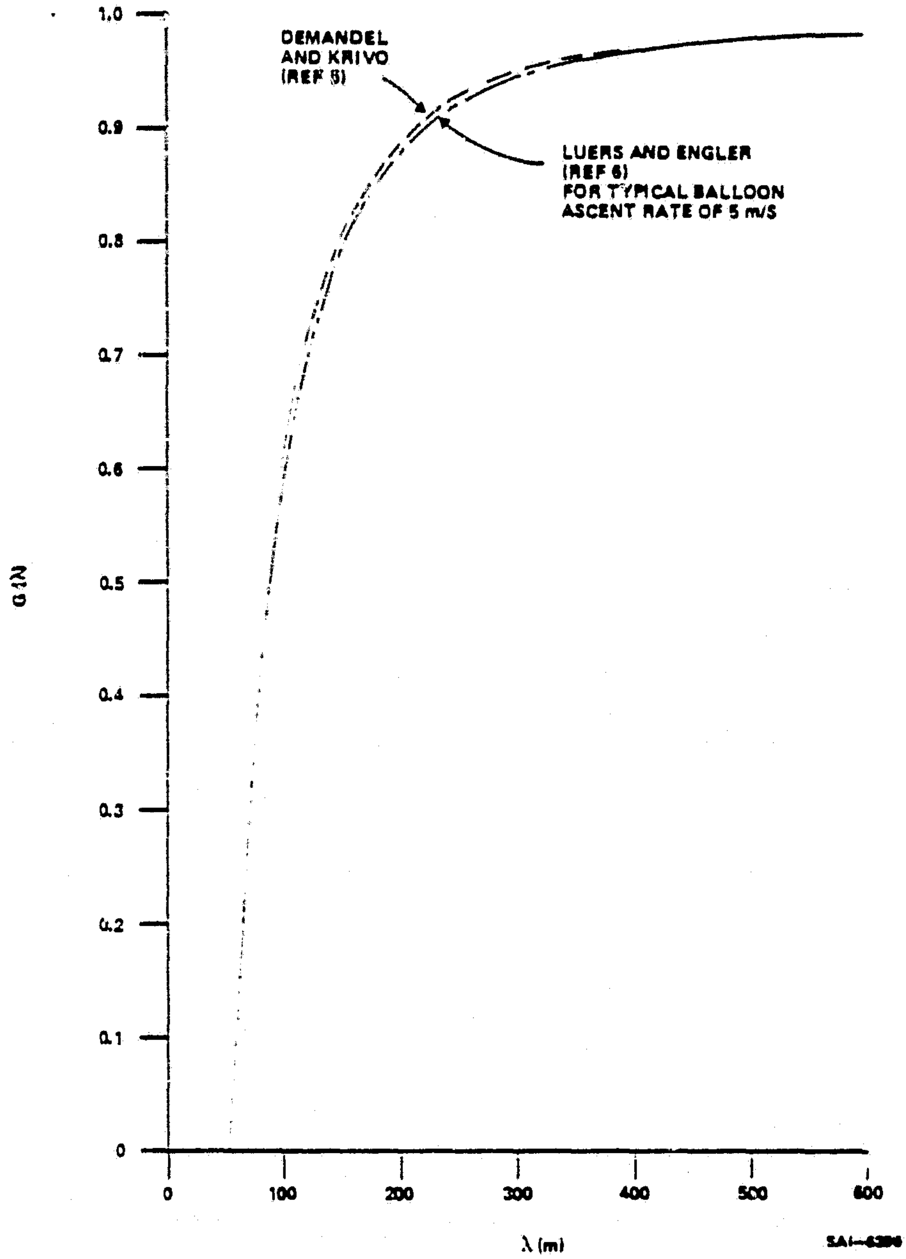

Figure 2. Amplitude Response of the Jimsphere System

D. <u>Filter Functions</u>.

Certain characteristics of winds aloft that are important in the planning and mission operations of space vehicles launched or retrieved at a particular location can be singled out for detailed study by application of specially designed digital filters to Jimsphere wind profiles.

The design of the digital filters is based on the Martin-Graham cosine rolloff model described by Demandel and Krivo (Ref. 7). A set of numerical smoothing weights is calculated for a low-pass filter from the equation

$$h(nT) = \frac{\sin(2\pi f_t nT) + \sin(2\pi f_c nT)}{2\pi nT\left[1 - 4n^2T^2(f_t - f_c)^2\right]} \qquad (5)$$

Where the filter design parameters are

- T = altitude interval of wind profile data
- n = weight index ($-N, -N+1, \ldots, -1, 0, 1, \ldots, N-1, N$)
- N = $(NW-1)/2$
- NW = number of weights
- f_c = cutoff frequency = the highest frequency with associated amplitude passed with <u>unity</u> gain
- f_t = termination frequency = the lowest frequency with associated amplitude passed with <u>zero</u> gain.

The center weight ($n = 0$) is given by:

$$h_o = f_c + f_t.$$

When the weights, h_n, have been determined, they are normalized by applying the constraint

$$\sum_{n=-N}^{N} h_n = 1. \qquad (6)$$

Only $(N + 1)$ weights are calculated since $h_n = h_{-n}$. Since the filter function is symmetrical, no phase shift is produced.

The use of digital smoothing weights results in the loss of the first and last N data points of the original profile. Thus the filtered wind profile has an altitude range that is reduced by 2NT compared to the original profile.

The effective response of the filter, given the design parameters listed under equation (5) is

$$G(f) = h_0 + 2 \sum_{n=1}^{N} h_n \cos(2\pi fnT) \quad , \tag{7}$$

As the number of weights (NW) is increased, the response of the filter improves. However, computation time increases as does the number of points lost (the first and last N data points). In this study NW was chosen to minimize data loss while maintaining a reasonably accurate filter response.

E. Filter Application.

Jimsphere wind profiles in component form (zonal and meridional) were decomposed into five data bases by the filtering process illustrated in Figure 3. The filter weights, h_i, and gain functions, G(f) calculated from equations 5 and 7 for low-pass filters I and II are listed in Tables 1 and 2, respectively. The power response of the filters, $G^2(f)$, illustrated in Figure 4 is a measure of the effect on the variance of the perturbations in the profile. For example, low-pass Filter I reduces the variance to 39.5 percent of its original value at a wavelength of 500 meters.

The effect of the filtering process on the zonal and meridional components of a particular profile is illustrated in Figures 5 and 6. The terms (steady state, residual I, wind bias, residual II and total residual) used to describe the data bases generated by the two-stage filtering process are defined below.

Steady state profiles are appropriate for analysis of winds aloft on the synoptic scale; these profiles represent average conditions over spatial scales of a few hundred kilometers in the horizontal and a few hundred meters in the vertical and temporal scales of a few hours.

The first residual profile (residual I) is calculated by subtraction of the steady state profile from the Jimsphere profile. This is analogous to the application of a high-pass filter having an amplitude response function that is the complement of the low-pass filter used to calculate the steady state wind profiles; i.e.,

$$G(f) \text{ high-pass} = 1 - G(f) \text{ low-pass} \tag{8}$$

The first residual profile contains the small wavelength perturbations in the Jimsphere profile that are not found in the steady state profile.

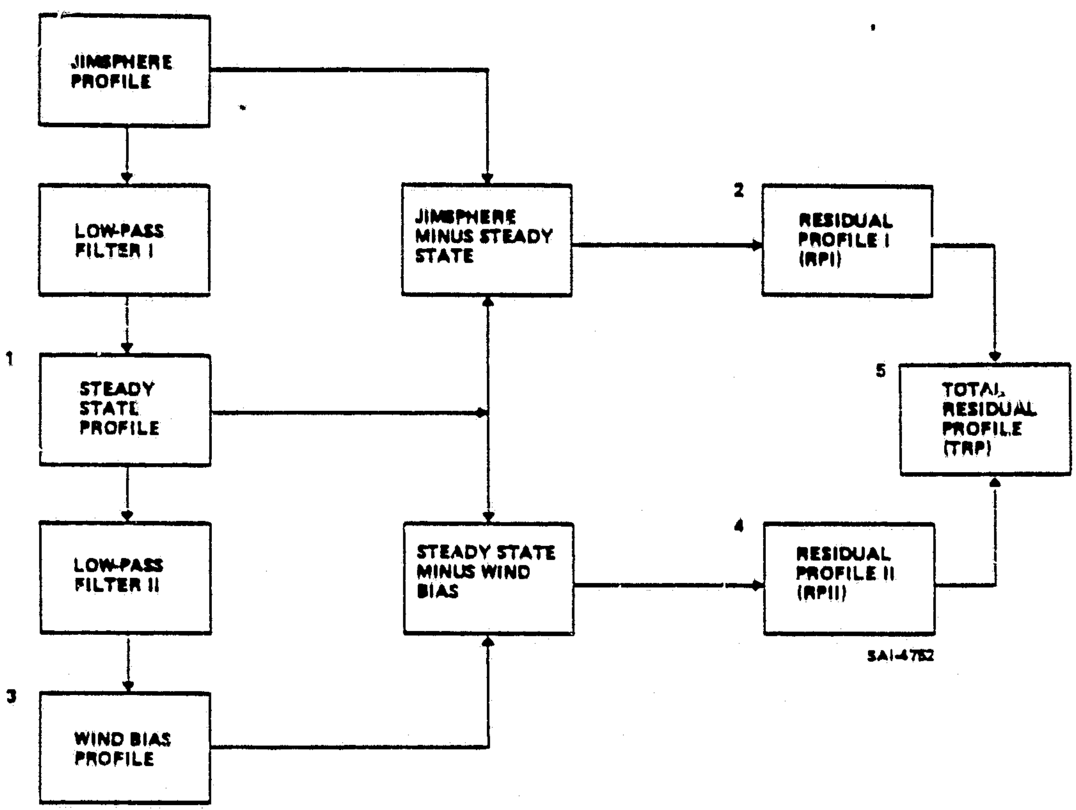

Figure 3. Digital Filtering of Jimsphere Profiles

TABLE 1. FILTER WEIGHTS, h_i, AND GAIN FUNCTION, G(f) OF LOW-PASS FILTER I FOR T=25 m, N=20, f_c=.00034 m^{-1} AND f_t=.00435 m^{-1}

Altitude	h_i	Filter Weight
Z_o (1)	h_o	.116360
$Z_o \pm 25$ m	$h_{+1,-1}$	.112682
$Z_o \pm 50$ m	$h_{+2,-2}$	.102183
"	"	.086370
"	"	.067415
"	"	.047750
"	"	.029618
"	"	.014711
"	"	.003949
"	"	-.002561
"	"	-.005395
"	"	-.005565
"	"	-.004229
"	"	-.002423
"	"	-.000884
"	"	.000021
"	"	.000259
"	"	.000022
"	"	-.000406
"	"	-.000771
$Z_o \pm 500$	$h_{+20,-20}$	-.000926

λ(m)	$f(m^{-1})$	G(f)
10,000	.0001	.9994
5,000	.0002	.9977
3,333	.0003	.9947
2,500	.0004	.9904
2,000	.0005	.9844
1,667	.0006	.9768
1,429	.0007	.9672
1,250	.0008	.9555
1,111	.0009	.9414
1,000	.001	.9249
500	.002	.6299
333	.003	.2512
250	.004	.0219
200	.005	-.0004
167	.006	-.0006
143	.007	.0008
125	.008	-.0009
111	.009	.0009
100	.010	-.0009

(1) Z_o = 500,525...19,500 m

TABLE 2. FILTER WEIGHTS, h_i, AND GAIN FUNCTION, G(f) OF LOW-PASS FILTER II FOR T=250 m, N=5, f_c=.00004 m^{-1} AND f_t=.00080 m^{-1}

Altitude	h_i	Filter Weight
Z_o (1)	h_o	.20333
$Z_o \pm 250$ m	$h_{+1,-1}$	.18260
$Z_o \pm 500$ m	$h_{+2,-2}$	.13008
"	"	.06865
"	"	.02065
$Z_o \pm 1250$ m	$h_{+5,-5}$	-.00365

λ(m)	$f(m^{-1})X10^{-4}$	G(f)
20,000	0.5	.9904
10,000	1	.9620
6,667	1.5	.9161
5,000	2	.8546
3,333	3	.6955
2,500	4	.5106
2,000	5	.3283
1,667	6	.1736
1,429	7	.0627
1,250	8	.0001
1,111	9	-.0210
1,000	10	-.0155

(1) Z_o = 1750,1775,...18,250 m

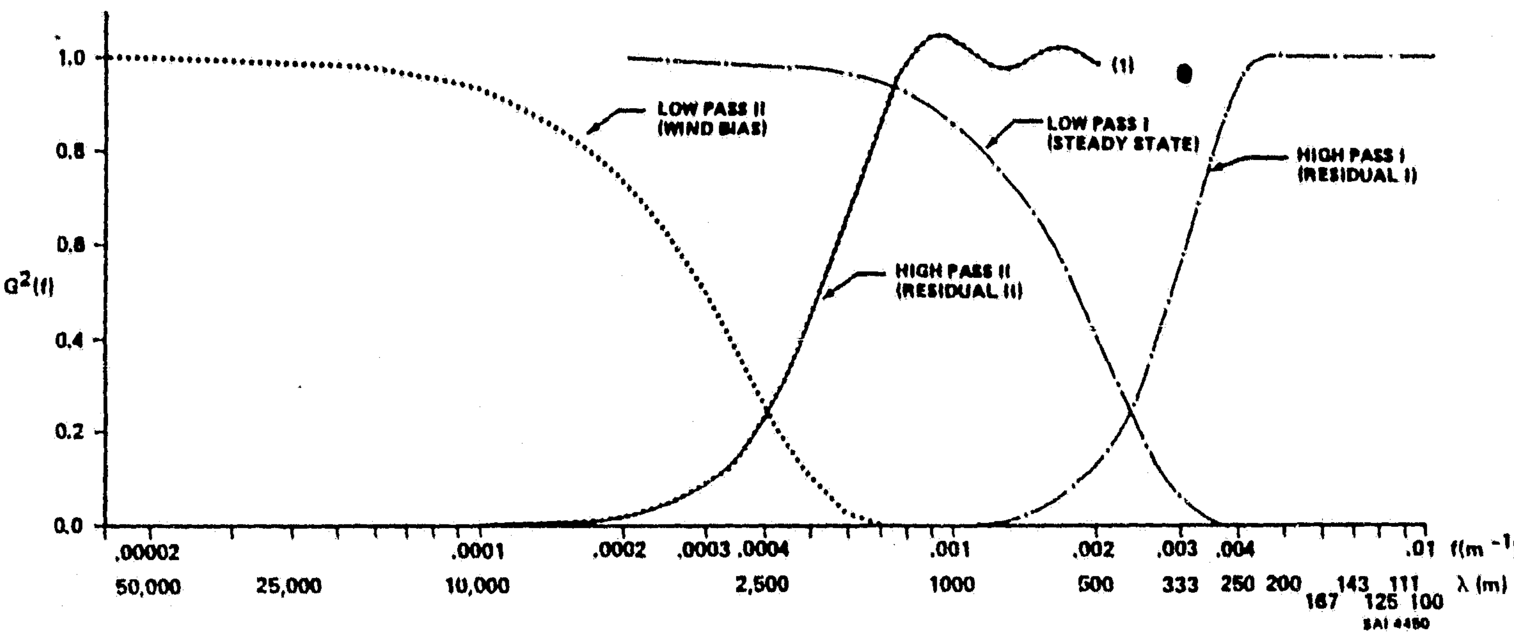

(1) DAMPED OSCILLATION; MAXIMUM AMPLITUDE LESS THAN 1.002 AT λ = 100 METERS.

Figure 4. Power Response of Digital Filters (I and II) and Associated Band-Pass of Filtered Profiles (Steady State, Residual I, Wind Bias and Residual II)

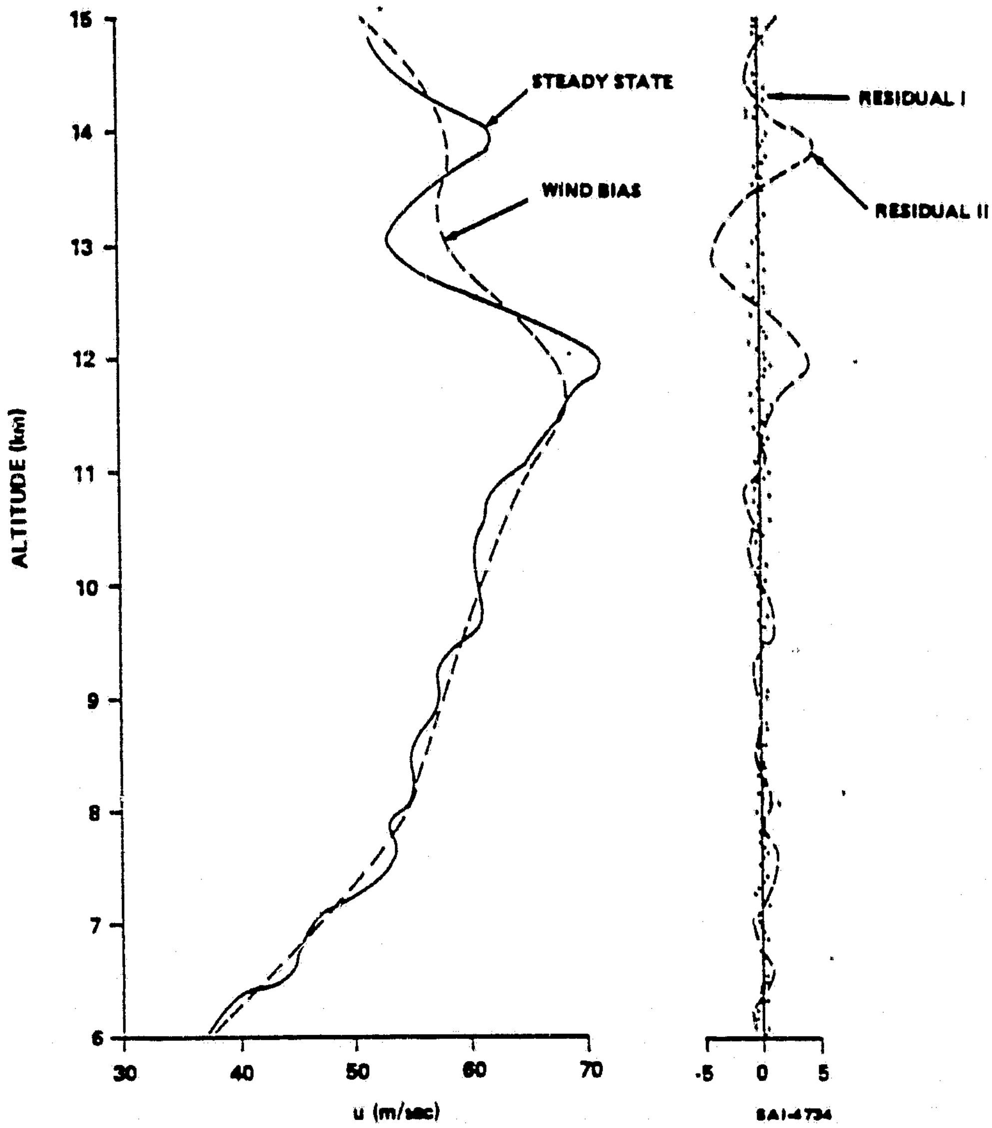

Figure 5. Filtered Profiles Calculated from Jimsphere Profile (Zonal Component) of 7 April 1966, 0955Z

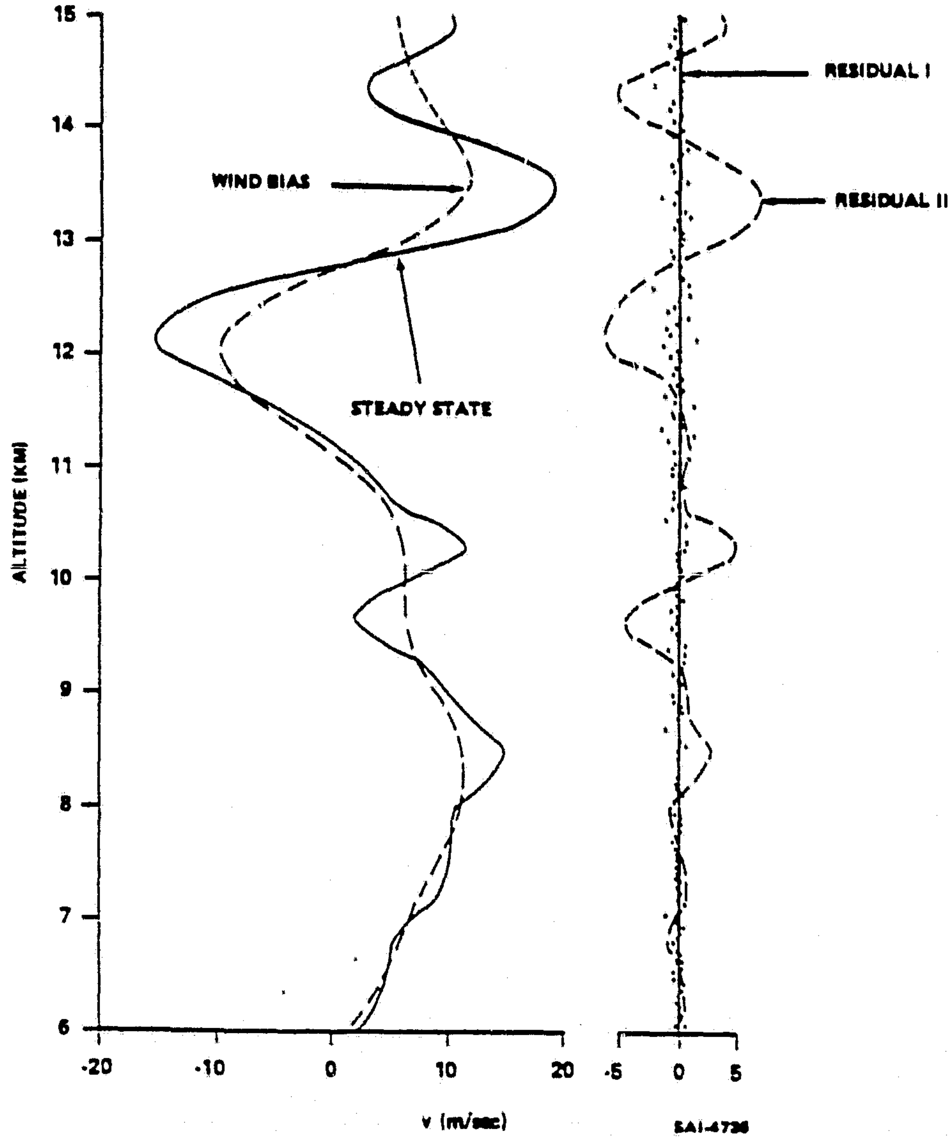

Figure 6. Filtered Profiles Calculated from Jimsphere Profile (Meridional Component) of 7 April 1966, 0955Z

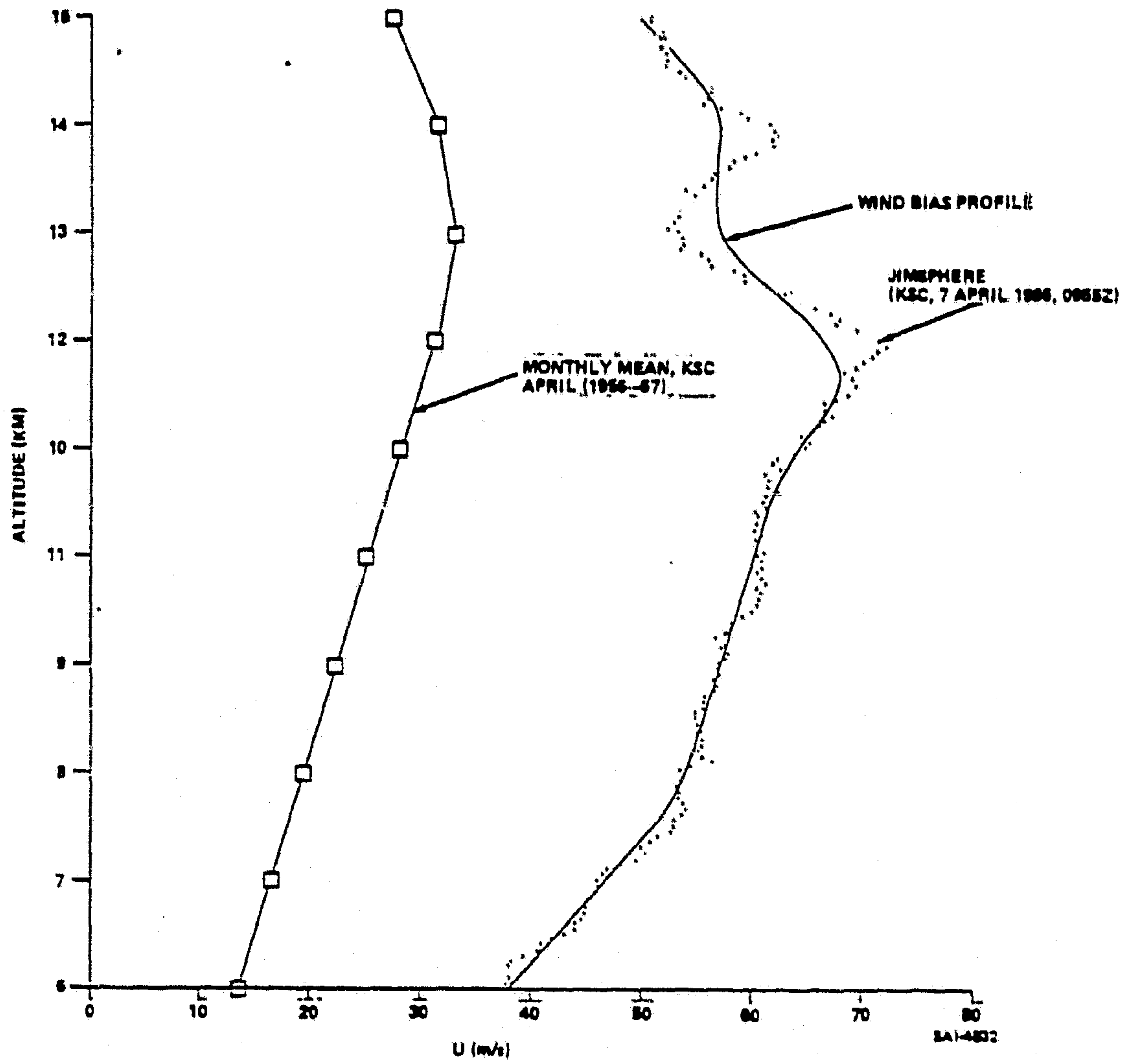

Figure 7. Wind Bias Profile Calculated from Jimsphere Profile and Artificial Profile Composed of Monthly Means for the Period 1956-67 at Cape Kennedy

Wind bias profiles emphasize the predominant large scale change in the wind from the surface to 20 km. Typically at Cape Kennedy, this large scale change is dominated by the maximum vector wind magnitude which occurs near 12 km. Steady state wind profiles clearly contain the large wavelength perturbations needed for wind biasing, but they also contain small wavelength perturbations that cannot be used. Wind bias profiles are calculated by application of a low-pass filter to the steady state profiles. The calculated wind profiles contain perturbation wavelengths similar to that found in a wind bias model based on the monthly mean wind. However, large differences of wind magnitude can occur between a particular wind bias profile and the monthly mean profile; this is illustrated in Figure 7. A filtered wind profile that is representative of the wind conditions associated with a particular launch is the most desirable basis for wind biasing of launch vehicles. The monthly mean profile is almost never representative of launch conditions. The filter function used to calculate the wind bias profiles could be used in future simulation studies or launch operations. The ultimate choice of an appropriate filter will be based on engineering considerations beyond the scope of this investigation.

The second residual profile (Residual II) contains the small scale perturbations in steady state wind profiles that are not required for wind biasing.

The total residual profile (Residual I + Residual II = TRP) contains all the perturbations that are of interest for analysis of vehicle response.

The wavelength limits of the various types of wind profile data are listed in Table 3; with exceptions noted in the table, the indicated wavelength corresponds to the wavelength at which the amplitude response of the appropriate filter (high-pass or low-pass) is equal to .50.

Table 3. Wavelength Limits for Jimsphere and Various Filtered Wind Profiles

	Wavelength Range (m)
Jimsphere	$90^{(1)} - \lambda_{max}^{(2)}$
Steady State	$420 - \lambda_{max}^{(2)}$
Residual I (RP I)	$90 - 420$
Wind Bias	$2{,}470 - \lambda_{max}^{(2)}$
Residual II (RP II)	$420 \quad 2{,}470$
Total Residual (TRP)	$90 - 2{,}470$

(1)Valve of λ for $G(\lambda)=0.5$ in equation (4)

(2)λ_{max} is equivalent for Jimsphere, steady state and wind bias profiles. The exact value of λ_{max} could be the subject of a detailed discussion which would not be pertinent to this report. If these profiles are subjected to a spectral analysis reliable estimates of the spectral energy could only be obtained at wavelengths considerably smaller than the length of the profile. However, a simple inspection of winds aloft statistical summaries and individual wind profiles leads to the conclusion that a wavelength somewhat larger than the length of a Jimsphere profile is detectable.

F. <u>Definition of Gust</u>

Let u' represent the zonal wind component at a specified reference altitude, H_o, in a residual profile. The zonal gust is defined as the maximum value of u' in the vicinity of altitude H_o with like sign to u' at H_o. The wavelength, λ, of the gust is defined as twice the altitude difference between the first zero crossing of u' detected by scanning upward and downward from the maximum value of u'. The altitudes of the zero crossings, H_2 and H_1, are calculated by linear interpolation according to

$$H_2 = H_{j-1} - \frac{25}{u'_j - u'_{j-1}} u'_{j-1} \qquad (9)$$

$$H_1 = H_{k+1} - \frac{25}{u'_{k+1} - u'_k} u'_{k+1} \qquad (10)$$

where H_2 = altitude of the first zero crossing for the <u>upward scan</u>

u'_{j-1} = last value of u' with like sign to sign of u' at H_o when scanning upward[1]

u'_j = first value of u' with sign opposite to sign of u' at H_o when scanning upward

H_{j-1} = altitude of u'_{j-1}

H_1 = altitude of the first zero crossing for the <u>downward scan</u>

u'_{k+1} = last value of u' with like sign to sign of u' at H_o when scanning downward

u'_k = first value of u' with sign opposite to sign of u' at H_o when scanning downward

H_{k+1} = altitude of u'_{k+1}

Substitution of v' for u' in the definition above yields the definition of the meridional gust component.

[1] The indices j and k increase upward

It follows from the definition of gust adopted for this study that a particular gust component (zonal or meridional) is independent of the other component. In most cases the altitude of the maximum speed associated with the gust and the wavelength of the gust will differ for the zonal and meridional components. The most realistic bivariate statistics of gusts and wind perturbations are obtained from the following combinations:

- Zonal component gust, u'_{max}, and associated meridional component perturbation, v', at the same altitude.

- Meridional component gust, v'_{max}, and associated zonal component perturbation, u', at the same altitude. The first combination is used in this study.

Thus, for any particular profile reference height we are considering, a wind vector which is composed of a gust or maximum of the zonal component near the reference height and an associated "perturbation" of the meridional component which is not necessarily the largest perturbation near the reference height.

The remaining alternative is the assumption that the zonal and meridional gusts (u'_{max} and v'_{max}) occur at the same altitude; this yields an unrealistically large value of the vector modulus; i.e.,

$$\begin{aligned} \sqrt{(u'_{max})^2 + (v'_{max})^2} &> \sqrt{(u'_{max})^2 + (v')^2} \\ \sqrt{(u'_{max})^2 + (v'_{max})^2} &> \sqrt{(u')^2 + (v'_{max})^2} \end{aligned} \qquad (11)$$

G. Gust Length

In connection with studies of gust gradient and wind shear, it is appropriate to define an altitude interval associated with a gust. This altitude interval defined as the gust length, L, is calculated by taking the altitude difference of the zero crossings on either side of the gust; i.e.,

$$L = H_2 - H_1 \qquad (12)$$

III. ANALYSIS

A. Maximum Vector Wind Modulus

The maximum vector wind modulus, R_{max}, is the largest wind speed, R, that can be found in a particular profile.

$$R = \sqrt{u^2 + v^2} \tag{13}$$

This section is concerned with an analysis of the probability distribution of R_{max}. A theoretical distribution is fitted to observed distributions of R_{max} for various types of filtered Jimsphere data.

R_{max} was calculated for each of the 150 profiles in each of the six data bases described in Section II.A. As illustrated in Figures 8 through 13, the probability distribution of R_{max} can be accurately represented by a gamma distribution of the form

$$Pr\left\{R_{max} \leq X\right\} = \frac{1}{\beta^{\gamma}\Gamma(\gamma)} \int_0^X x^{\gamma-1} EXP\ (-x/\beta)dx \tag{14}$$

$$\text{for } \beta > 0,\ \gamma > 0$$

where the parameters γ and β are functions of the mean, $\overline{x}$, and standard deviation, σ, of R_{max}.

$$\gamma = (\overline{x}/\sigma)^2 \tag{15}$$

$$\beta = \frac{\overline{X}}{\gamma} \tag{16}$$

The integral in Equation 14 is evaluated by a numerical approximation utilizing Simpson's rule.

Table 4 contains a list of statistics pertinent to the calculation of the theoretical probability distributions of R_{max} utilizing Equation 14. Various percentiles from the observed probability distributions of R_{max} during April are given in Table 5.

As illustrated in Figures 14 and 15, γ (dimensionless) and β (m/s) can be estimated from λ_m(km) according to

$$\gamma = 27.269 - 4.240 \ln \lambda_m \quad (\lambda_m \geq .125 \text{ km}) \tag{17}$$

$$\beta = .140\ \lambda_m^{.851} \tag{18}$$

where, λ_m is a measure of the largest wavelength in a particular type of wind profile. For residual profiles (I, II and total), λ_m is

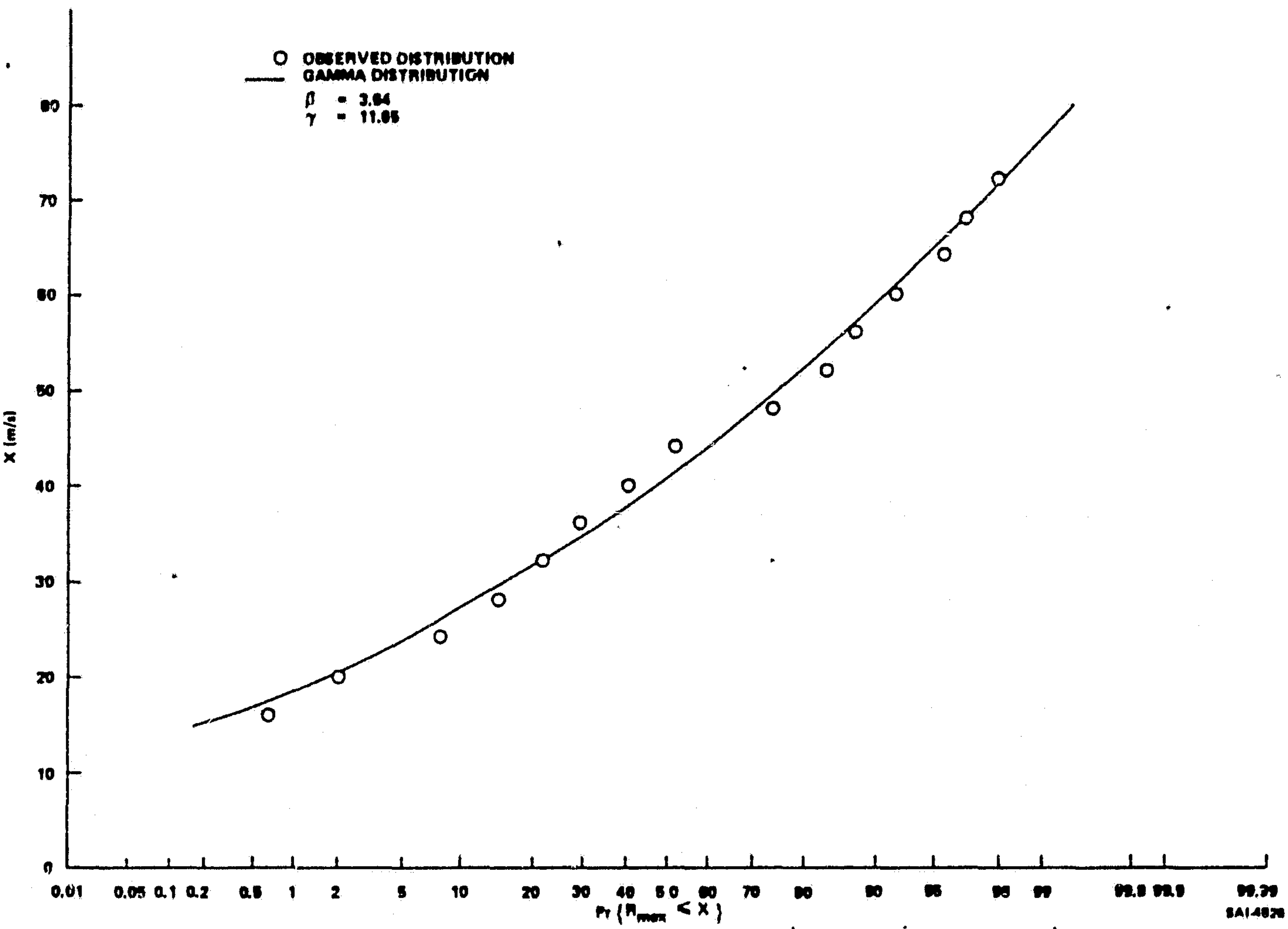

Figure 8. Observed and Theoretical (Gamma) Distribution of Maximum Vector Modulus, R_{max}, in Jimsphere Profiles During April at Cape Kennedy

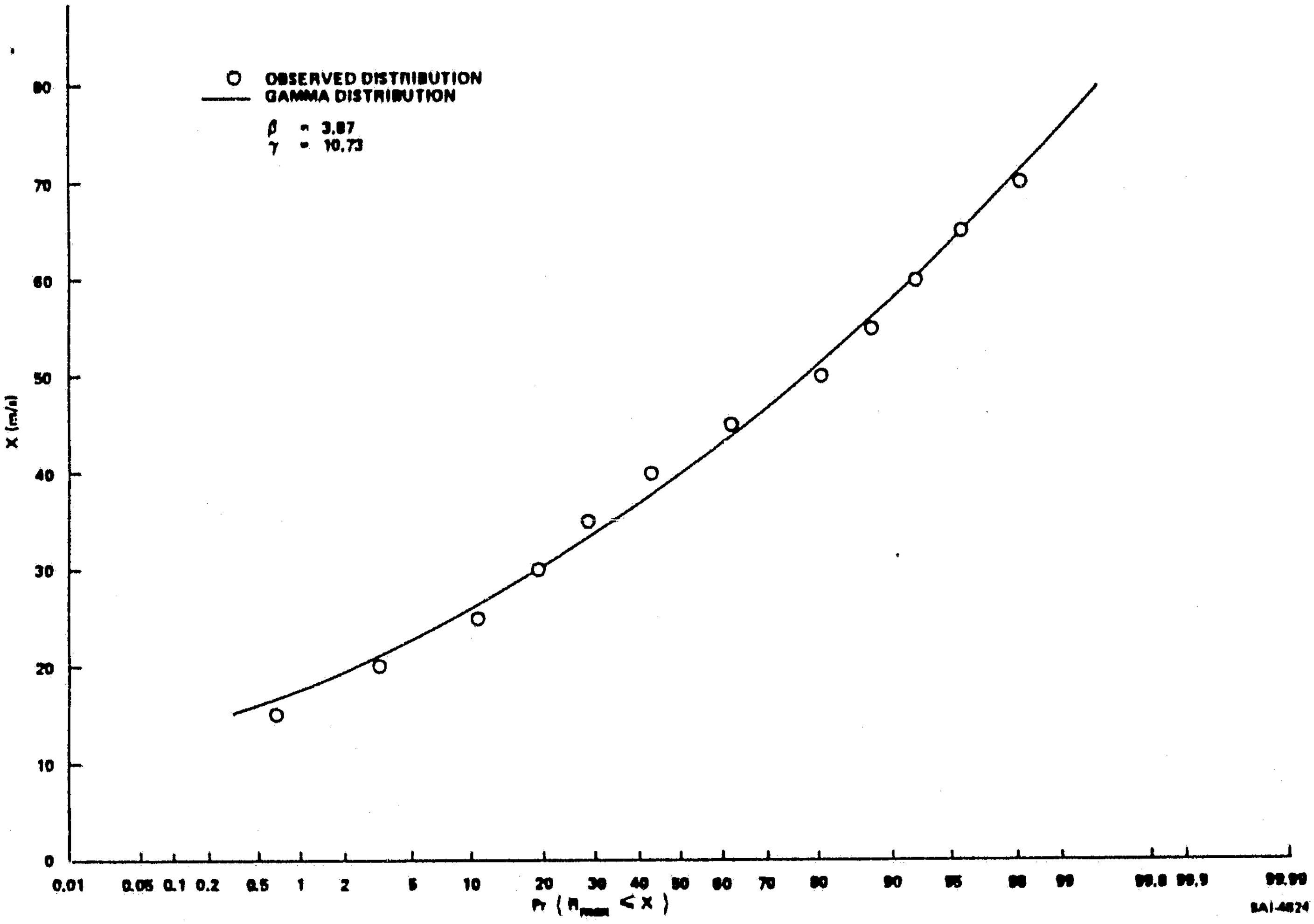

Figure 9. Observed and Theoretical (Gamma) Distribution of Maximum Vector Modulus, R_{max}, in Steady State Profiles During April at Cape Kennedy

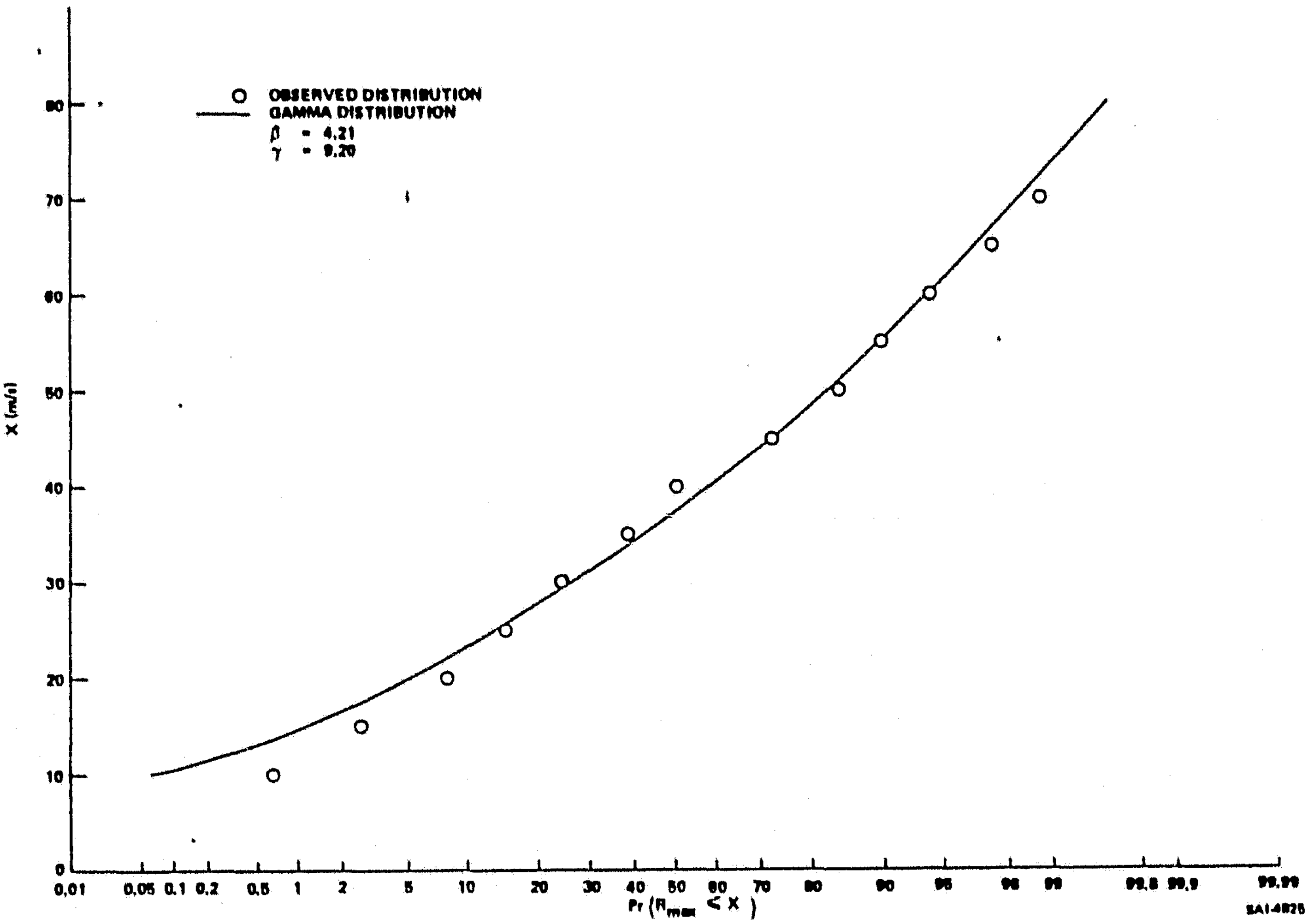

Figure 10. Observed and Theoretical (Gamma) Distribution of Maximum Vector Modulus, R_{max}, in Wind Bias Profiles During April at Cape Kennedy

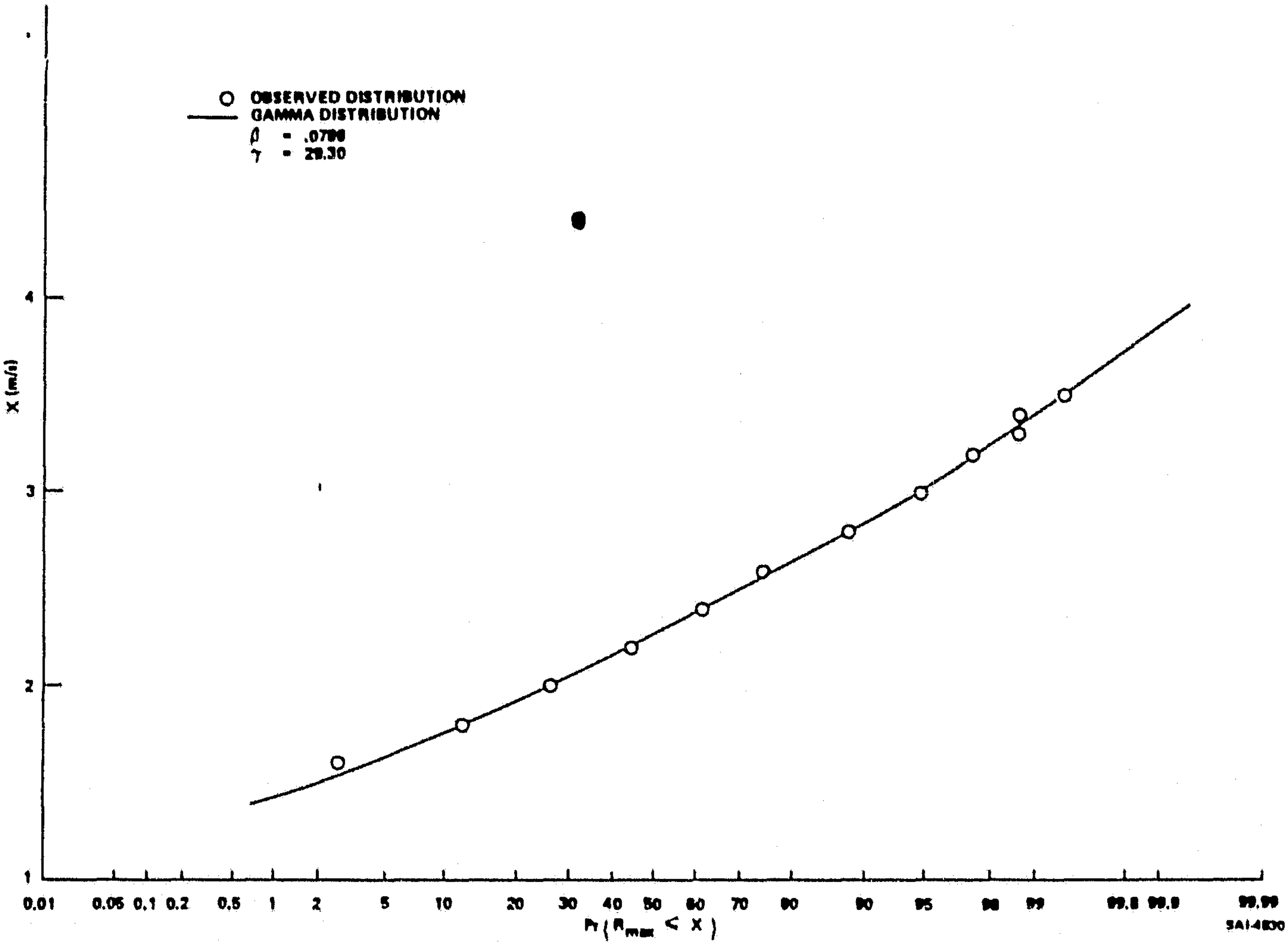

Figure 11. Observed and Theoretical (Gamma) Distribution of Maximum Vector Modulus, R_{max}, in Residual I Profiles During April at Cape Kennedy

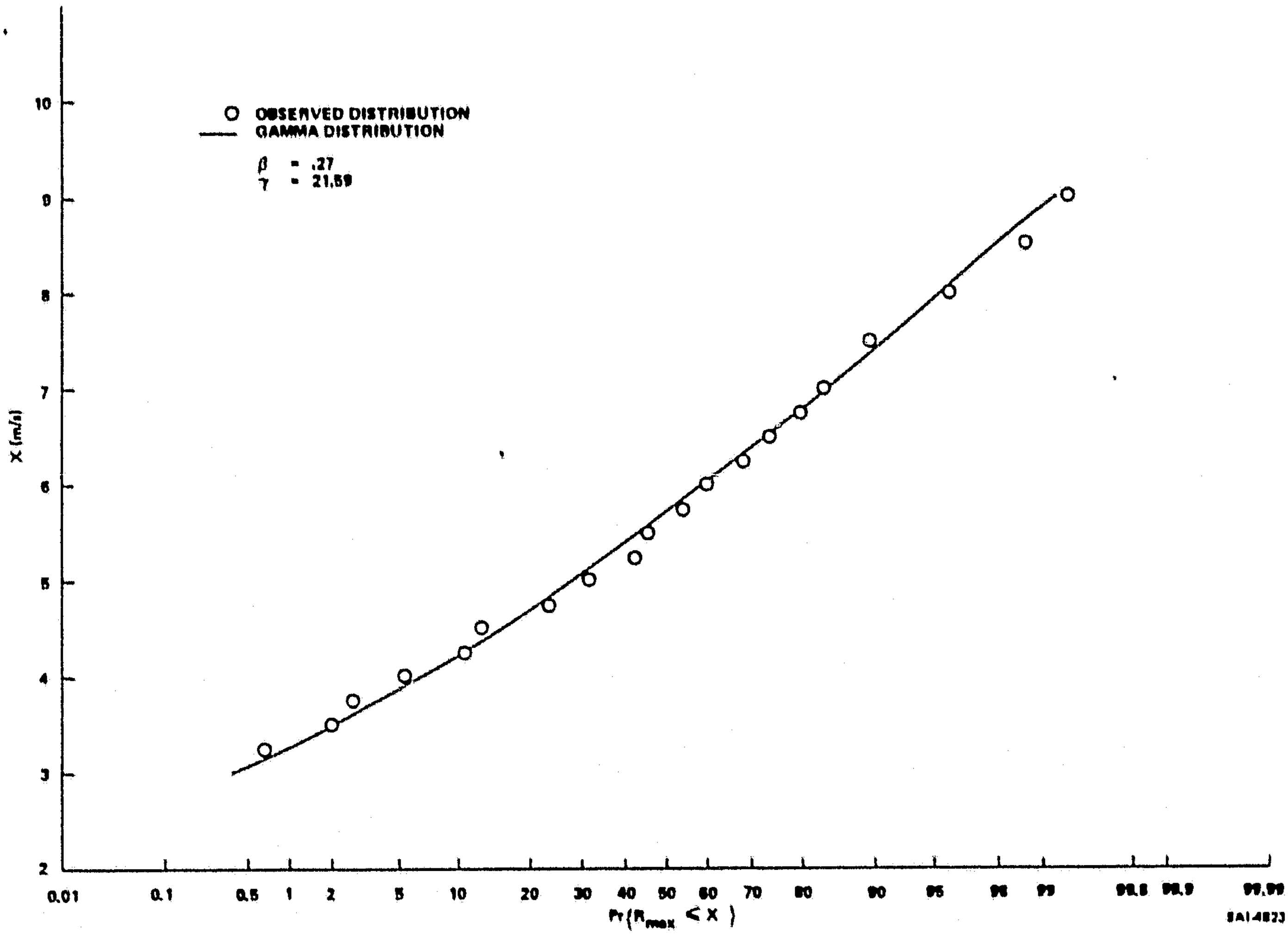

Figure 12. Observed and Theoretical (Gamma) Distribution of Maximum Vector Modulus, $\mathcal{R}_{max}$, in Residual II Profiles During April at Cape Kennedy

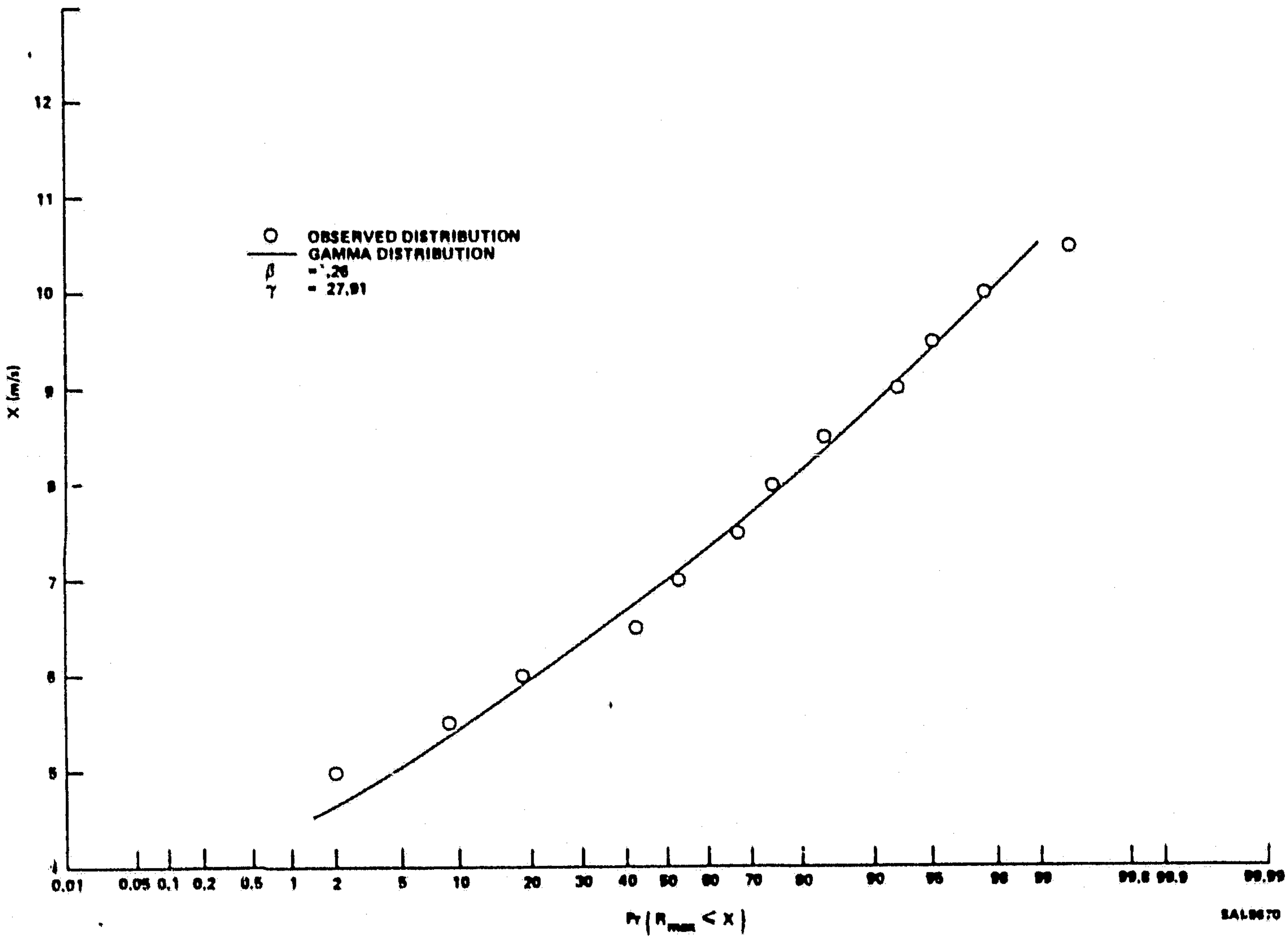

Figure 13. Observed and Theoretical (Gamma) Distribution of Maximum Vector Modulus, R_{max}, in Total Residual Profiles During April at Cape Kennedy

TABLE 4. MEAN, $\overline{X}$, AND STANDARD DEVIATION, σ, OF R_{max} AND THE PARAMETERS β and γ OF THE GAMMA DISTRIBUTION OF R_{max} AND THE PARAMETER λ_m USED IN EQUATIONS 11 and 12, APRIL, CAPE KENNEDY

Data Base	$\overline{X}$ (m/s)	σ (m/s)	β (m/s)	γ (dimensionless)	λ_m (km)
Jimsphere	42.36	12.41	3.64	11.65	48(1)
Steady State	41.51	12.67	3.87	10.73	48(1)
Wind Bias	38.78	12.78	4.21	9.20	48(1)
Total Residual	7.11	1.35	.26	27.91	2.47
Residual II	5.77	1.24	.27	21.59	2.47
Residual I	2.30	.426	.0786	29.30	.42

(1) Estimated; refer to succeeding paragraphs of text

TABLE 5. PERCENTILES FROM THE OBSERVED PROBABILITY DISTRIBUTIONS OF R_{max} DURING APRIL AT KSC

	R_{max} (m/s)				
Data Base	50	80	90	95	99 Percentile
Jimsphere	41	52	59	65	76
Steady State	40	52	58	64	76
Wind Bias	37	49	56	62	74
Total Residual	6.9	8.3	8.9	9.5	10.3
Residual II	5.7	6.8	7.4	7.9	8.9
Residual I	2.3	2.7	2.9	3.0	3.4

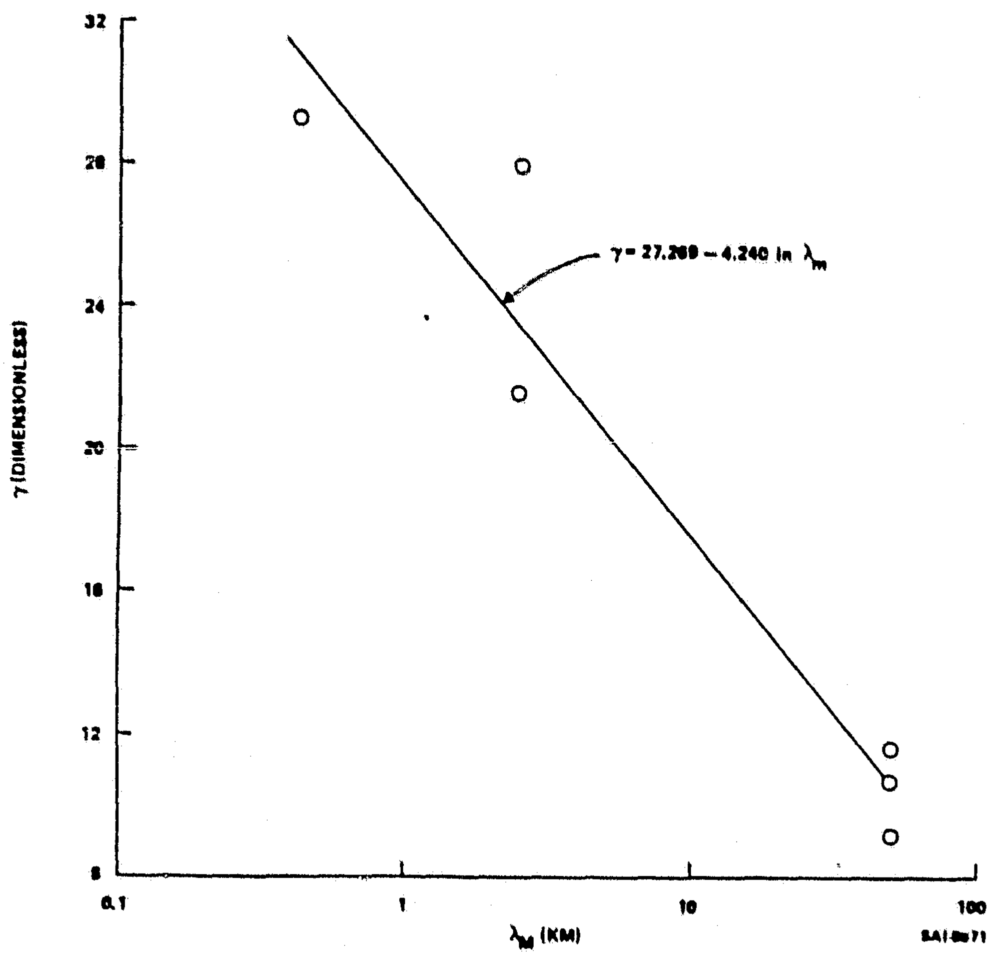

Figure 14. Parameter $\dot{\gamma}$ as a Function of λ_m (Cape Kennedy, April, R_{max})

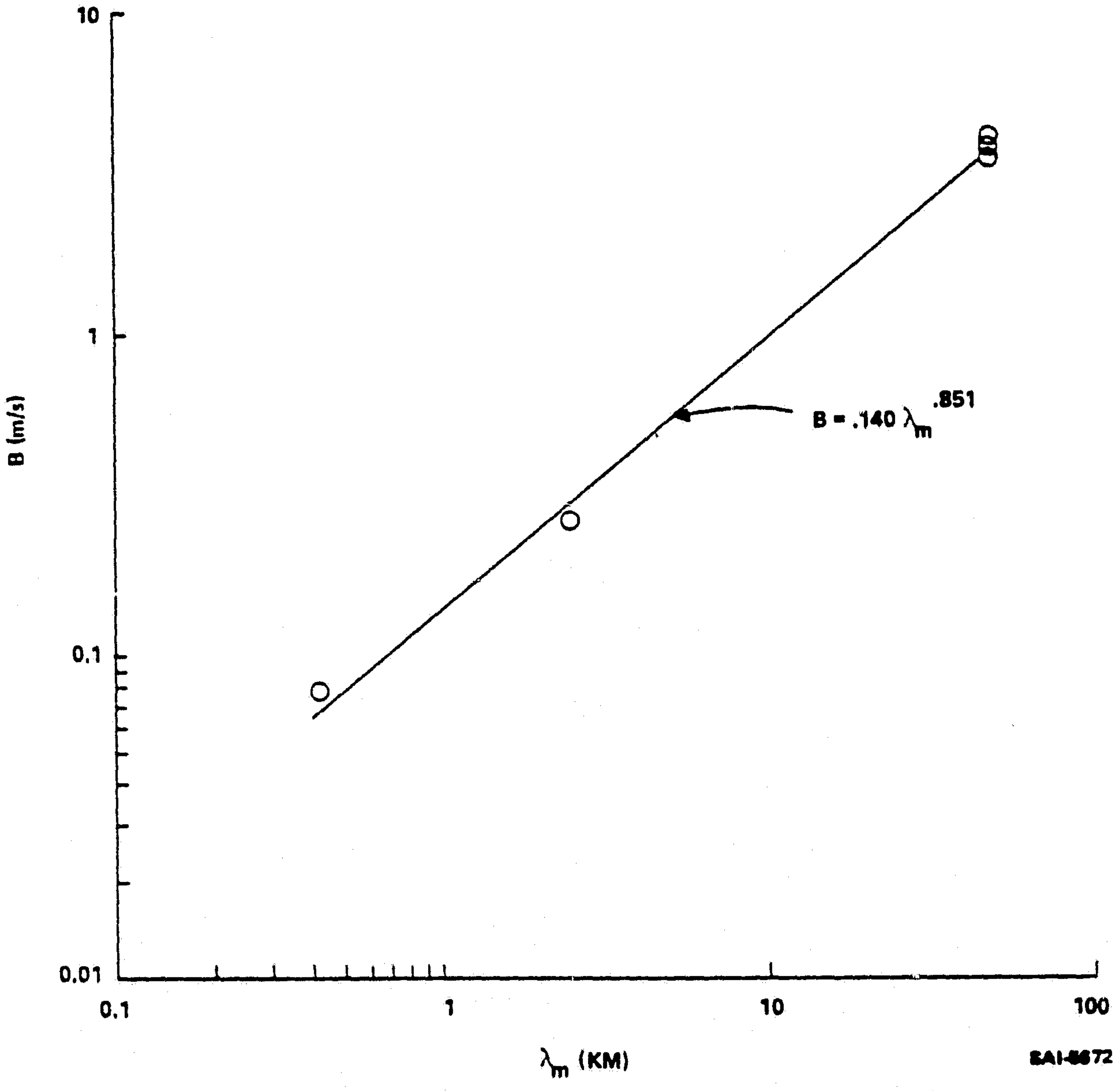

Figure 15. Parameter β as a Function of λ_m (Cape Kennedy, April, R_{max})

the wavelength at which the amplitude response of the high-pass filter is equal to .50. For wind profiles dominated by a large wavelength component (Jimsphere, steady state and wind bias profiles), λ_m cannot be specified from a known filter function. However, an estimate of λ_m can be obtained by assuming that the average altitude (~12 km) of R_{max} for these profiles is $\lambda_m/4$; thus λ_m = 48 km. It must be pointed out that the validity of equations 16 and 17 is dependent on the validity of the assumption described above. Therefore, the estimation of the parameters γ and β utilizing Equations 17 and 18 could become inaccurate for λ_m greater than 2.47 km.

A comparison of R_{max} probability distributions for April and February for two types (TRP and II) of filtered profiles is illustrated in Figure 16. It is indicated that the differences between the distribution attributable to month are small compared to differences attributable to wavelength range (filter type). The TRP profiles contain wavelengths between 90 and 420 m which are not contained in Residual II profiles. At the 99 percentile level, these wavelengths contribute 1.6 to 1.8 m/sec to the distribution of R_{max} calculated from TRP data; at smaller percentiles the contribution is slightly smaller.

Probability distributions of the altitude, Z_{max} of the maximum modulus calculated from April data are illustrated in Figures 17 thru 20. Percentiles of Z_{max} are listed in Table 6. It is concluded that

- Z_{max} is largest for residual profiles
- The distributions of Z_{max} for wind profiles dominated by the same large wavelength component (Jimsphere, steady state and wind bias profiles) are nearly equivalent.

TABLE 6. PERCENTILES OF Z_{max} ASSOCIATED WITH R_{max} DURING APRIL AT CAPE KENNEDY

R_{max} (m/sec)

Data Base	50	80	90	95	99 Percentile
Jimsphere	13.1	13.9	14.4	15.2	15.9
Steady State	13.1	13.9	14.4	15.2	15.8
Wind Bias	12.9	13.8	14.4	15.1	15.9
Residual II	14.4	16.1	16.9	17.2	17.7
Residual I	16.0	17.0	17.3	17.5	17.9

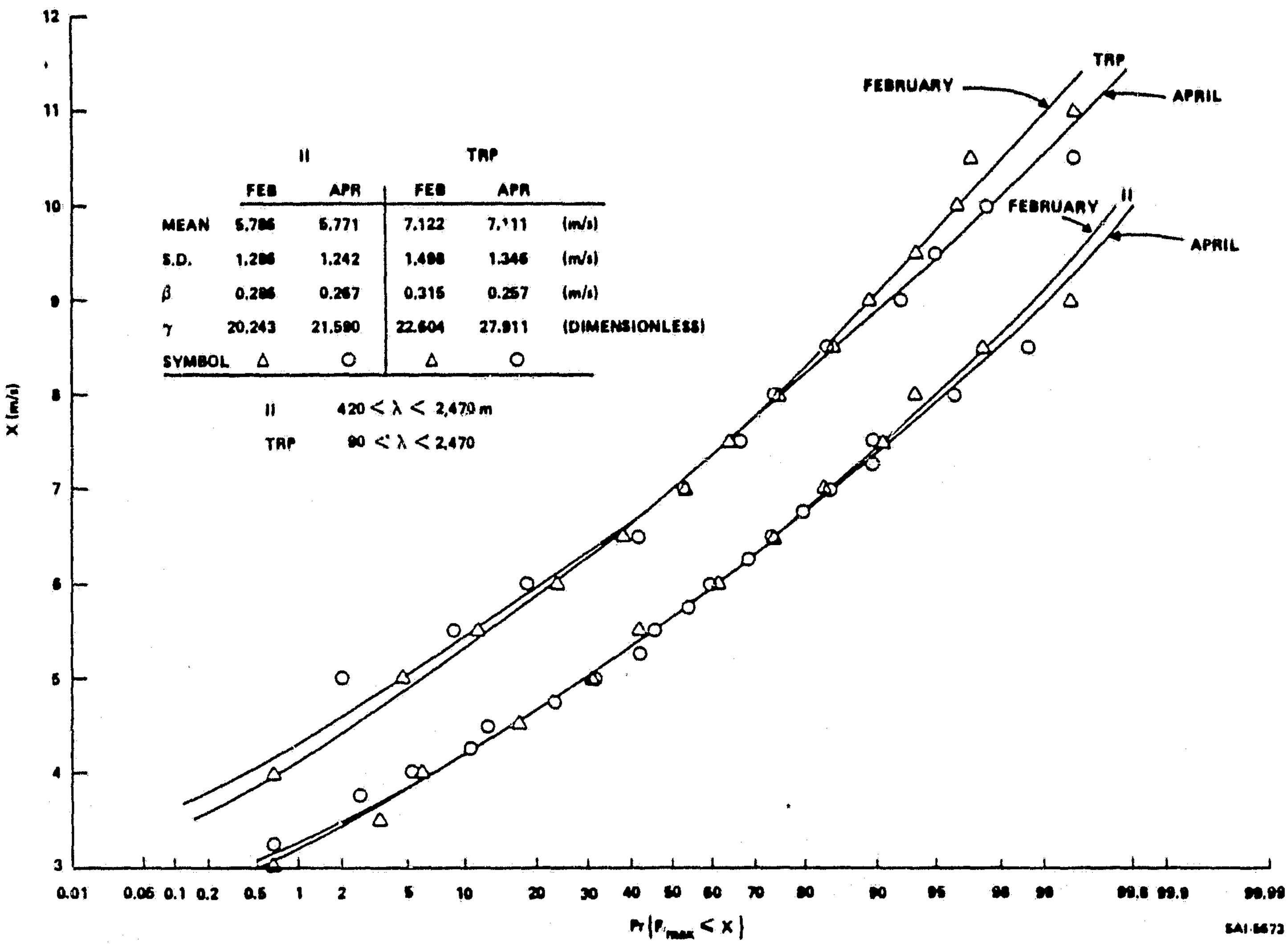

Figure 16. Theoretical (Gamma) and Observed Distribution of Maximum Gust Modulus, R_{max}, During February and April at Cape Kennedy

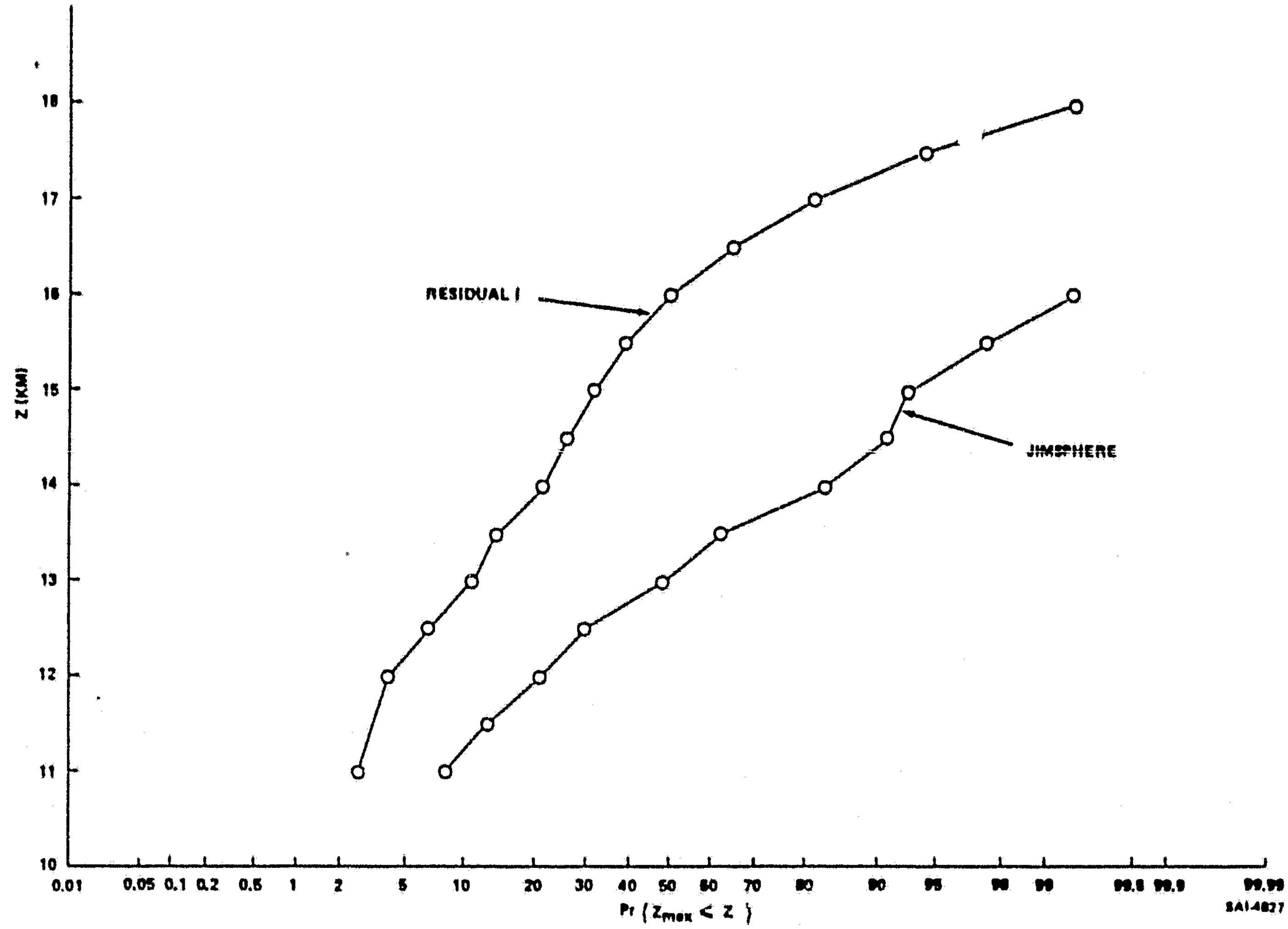

Figure 17. Observed Distribution of Z_{max} for Residual I and Jimsphere Profiles During April at Cape Kennedy

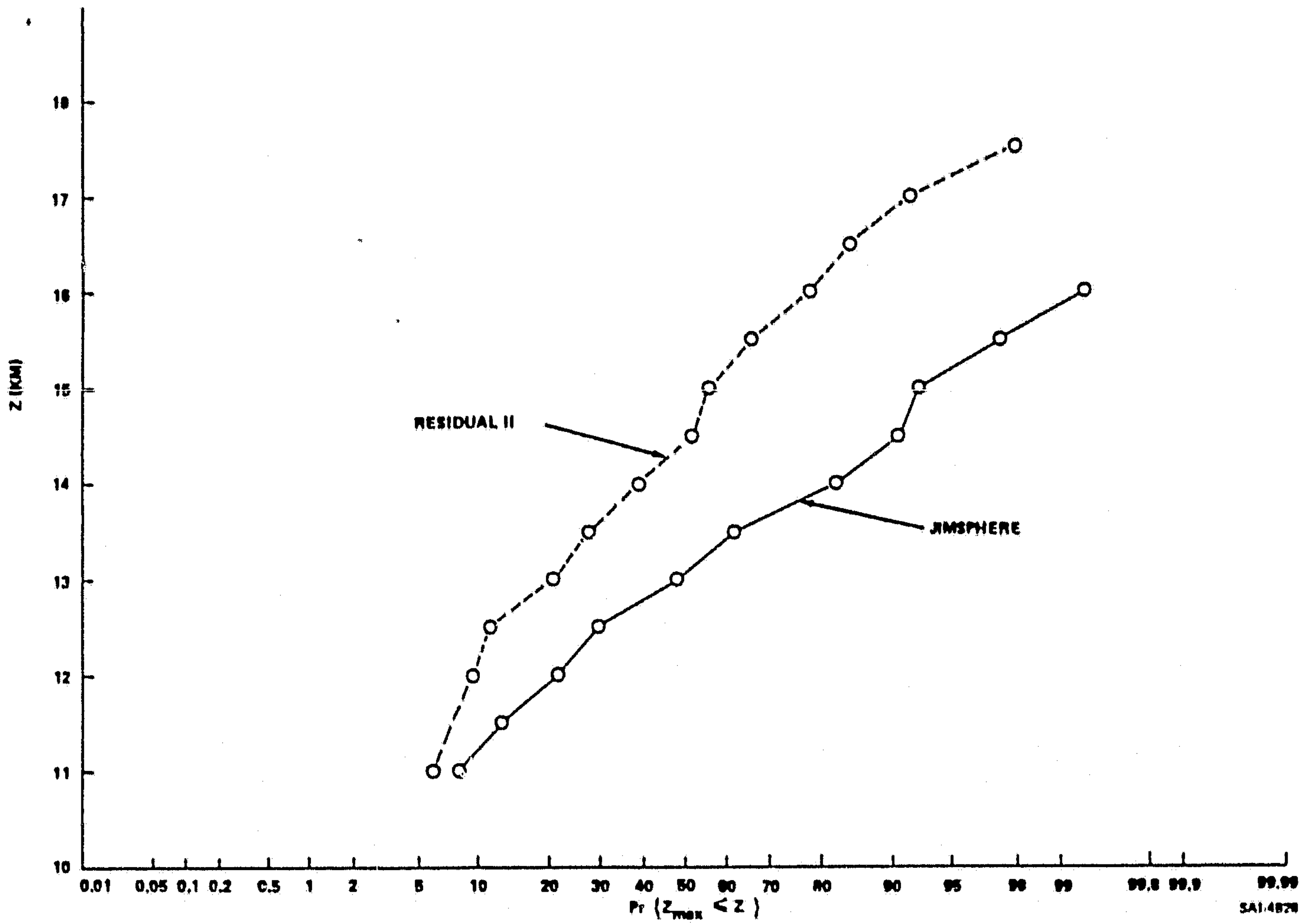

Figure 18. Observed Distribution of Z_{max} for Residual II and Jimsphere Profiles During April at Cape Kennedy

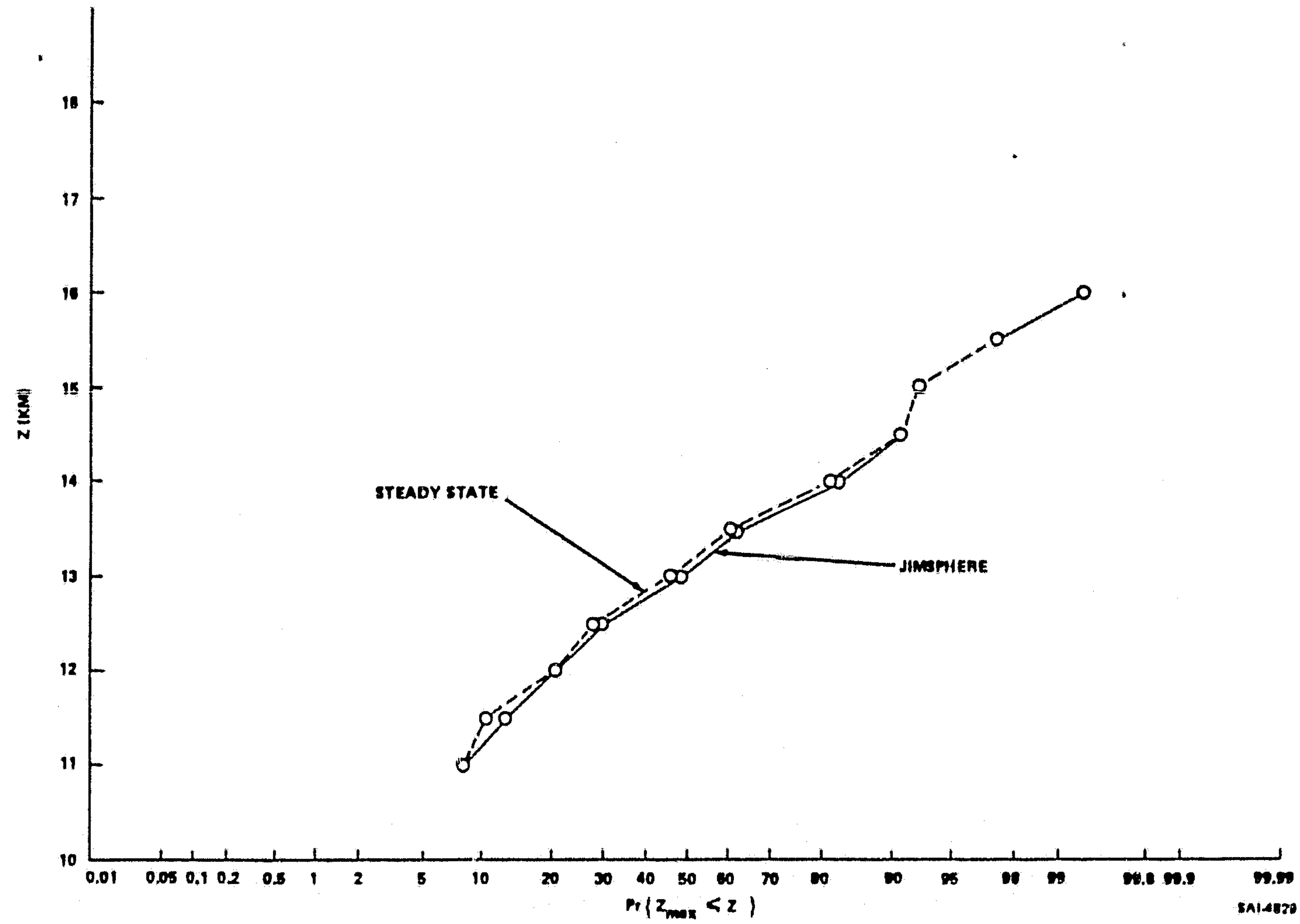

Figure 19. Observed Distribution of Z_{max} for Steady State and Jimsphere Profiles During April at Cape Kennedy

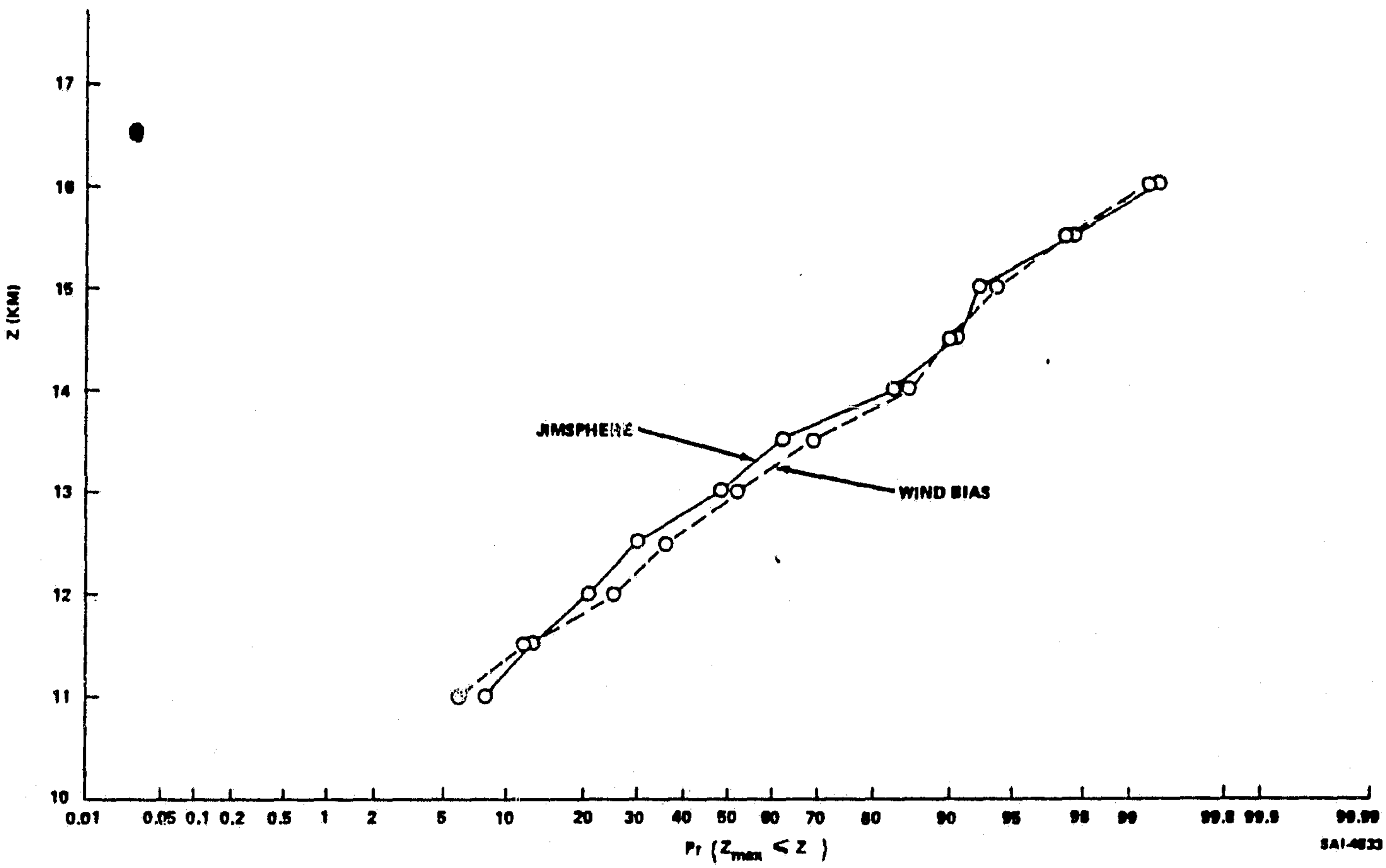

Figure 20. Observed Distribution of Z_{max} for Wind Bias and Jimsphere Profiles During April at Cape Kennedy

B. Gust Vector Modulus

A large body of statistics indicating the variation of gust vector modulus, R, with altitude (6 to 14 km), month (February and April), and filtered profile type have been generated in this study. An analysis of the statistics has led to the following conclusions:

- The probability distribution of R at a particular reference altitude is strongly related to the strength of the large wavelength component in the wind profiles. A comparison of probability distributions of R, at KSC during April at 12 km, for two wavelength ranges is illustrated in Figure 21. A reasonable upper limit for R at 12 km in the wavelength range from 90 to 420 m is 3 m/sec; in comparison, a value of 8.5 m/sec is estimated for the wavelength range from 420 to 2,470m.

- Gust modulus at 12 km in the 420 to 2,470m wavelength range is somewhat larger during February in comparison to April at KSC. As illustrated in Figure 22, the observed distributions diverge at the large percentiles.

- Gust modulus calculated from total residual profiles (125 $(90 < \lambda < 2470\text{m})$ increases with altitude between 6 and 14 km. As illustrated in Figure 23, the rate of increase is largest between 10 and 12 km.

Percentiles calculated from the observed probability distribution of gust vector modulus from total residual profiles at various reference altitudes are listed in Table 7.

C. Gust Vector Modulus Associated with Maximum Wind Speed and Maximum Vector Shear[1]

Distributions of gust modulus $(90 < \lambda < 2470\text{m})$ associated with maximum wind modulus and maximum vector shear in unfiltered Jimsphere profiles are illustrated in Figures 24 and 25, respectively. Gust data for the distributions were obtained at the altitudes of maximum wind speed and at the altitudes of the top of the layer of maximum shear for shear layer thicknesses of 100, 500 and 1,000m.

---

[1] The equation for maximum vector shear, w_{max}, is

$$w_{max} = \left(\sqrt{(\Delta u)^2 + (\Delta v)^2}\right)_{max}$$

where Δu and Δv are calculated over a layer thickness, Δz.

Table 7. Observed Percentiles of Gust Vector Modulus for Total Residual Profiles ($90 < \lambda < 2,470$m) at Cape Kennedy

X (m/sec)

Pr {R ≤ X} (PERCENT)	6 KM FEB	6 KM APR	8 KM FEB	8 KM APR	10 KM FEB	10 KM APR	12 KM FEB	12 KM APR	14 KM FEB	14 KM APR
1	0.25	0.32	0.10	0.37	0.35	0.22	0.30	0.47	0.55	0.27
2.5	0.43	0.57	0.27	0.43	0.52	0.29	0.47	0.56	0.84	0.74
5	0.58	0.71	0.52	0.49	0.77	0.47	0.85	0.68	1.02	1.28
10	0.76	0.96	0.82	0.70	1.00	0.70	1.27	1.10	1.47	1.60
20	1.09	1.28	1.17	1.10	1.40	0.99	1.86	1.50	2.20	2.46
40	1.76	1.80	1.80	1.55	1.84	1.52	2.57	2.40	3.00	3.71
50	1.97	2.04	2.10	1.83	2.17	1.70	3.06	2.80	3.46	3.95
60	2.22	2.30	2.43	2.10	2.50	1.83	3.50	3.19	3.78	4.30
80	2.89	2.83	2.97	2.80	3.31	2.61	5.00	4.07	4.87	5.45
90	3.12	3.40	3.80	3.13	4.20	3.06	6.80	4.80	5.90	6.35
95	3.84	3.82	3.92	3.42	4.90	3.82	7.15	5.32	6.70	7.62
97.5	4.03	4.08	4.26	4.23	5.65	4.03	7.65	6.63	7.13	8.33
99	4.30	4.35	4.37	4.85	6.15	4.65	8.50	6.85	8.70	9.17

SAI-8904

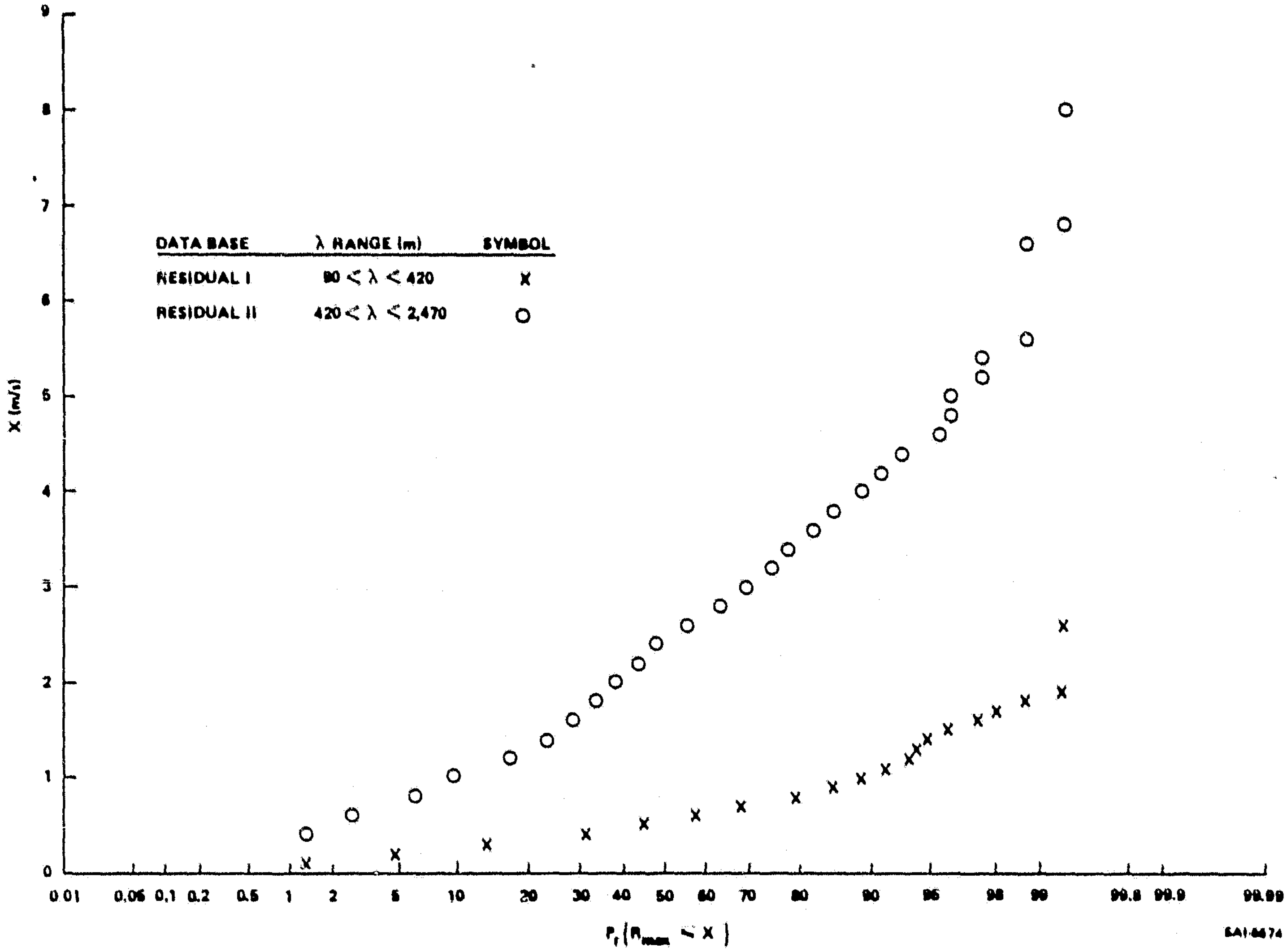

Figure 21. Observed Distribution of Gust Modulus, R, at 12 km During April at Cape Kennedy

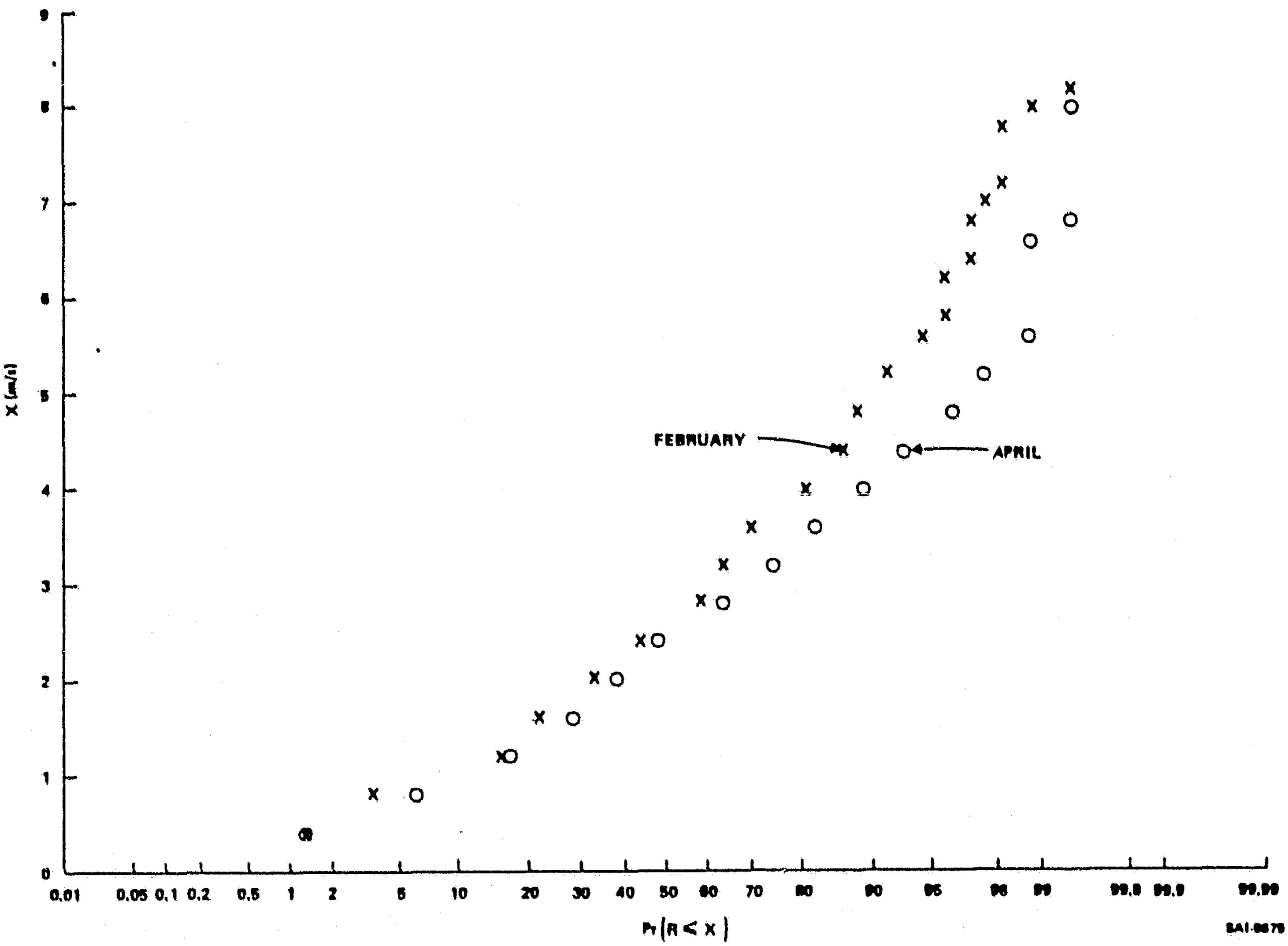

Figure 22. Observed Distribution of Gust Modulus, R, Calculated from Residual II Profile Data (420<λ<2,470m) at 12 km during February and April at Cape Kennedy

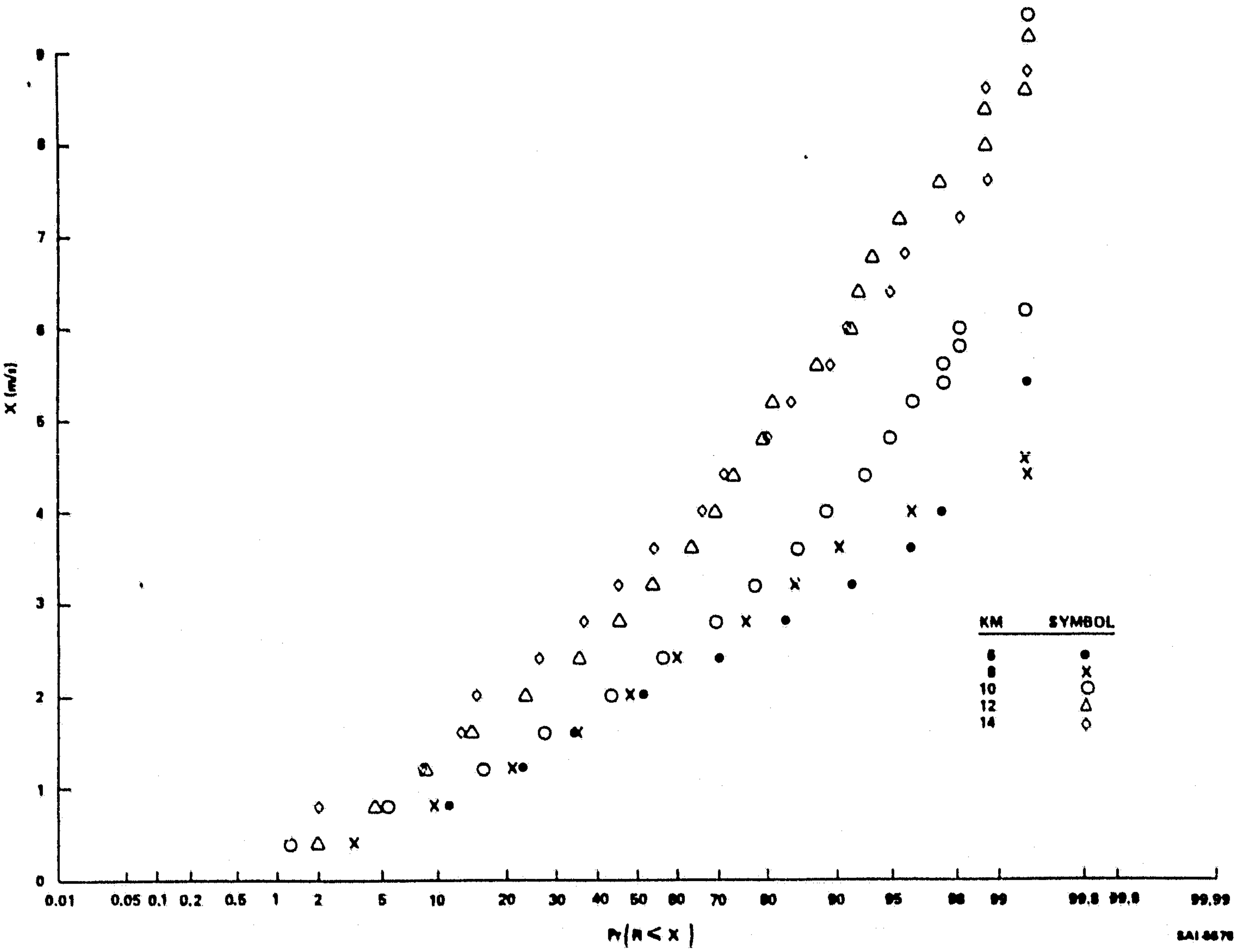

Figure 23. Observed Distribution of Gust Modulus, R, Calculated From Total Residual Profile Data (90<λ<2,470m) at 6, 8, 10, 12 and 14 km During February at Cape Kennedy

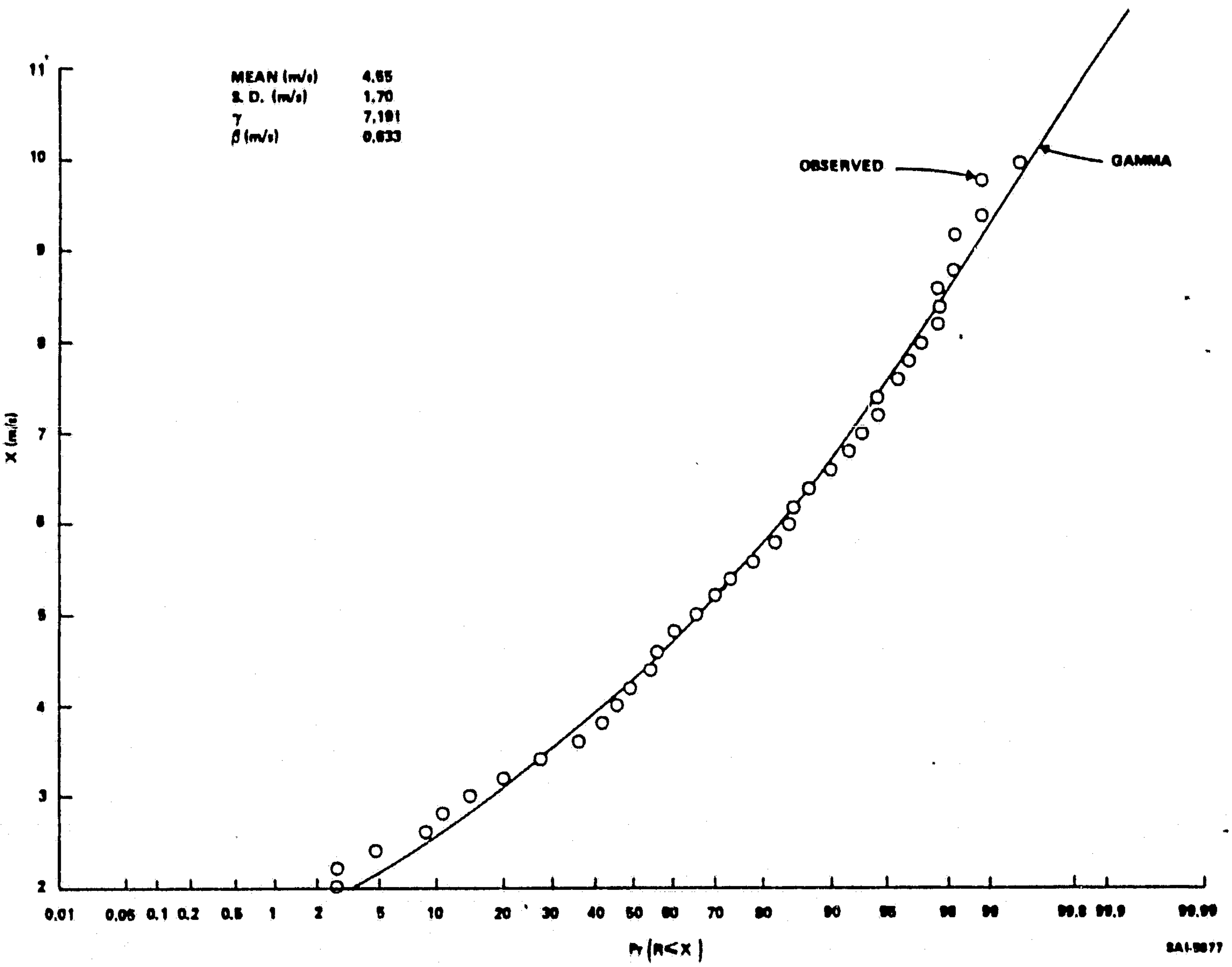

Figure 24. Observed and Theoretical (Gamma) Distribution of Gust (90<λ<2,470m) Modulus, R, Associated with Altitude of Maximum Wind in Jimsphere Profiles During April at Cape Kennedy

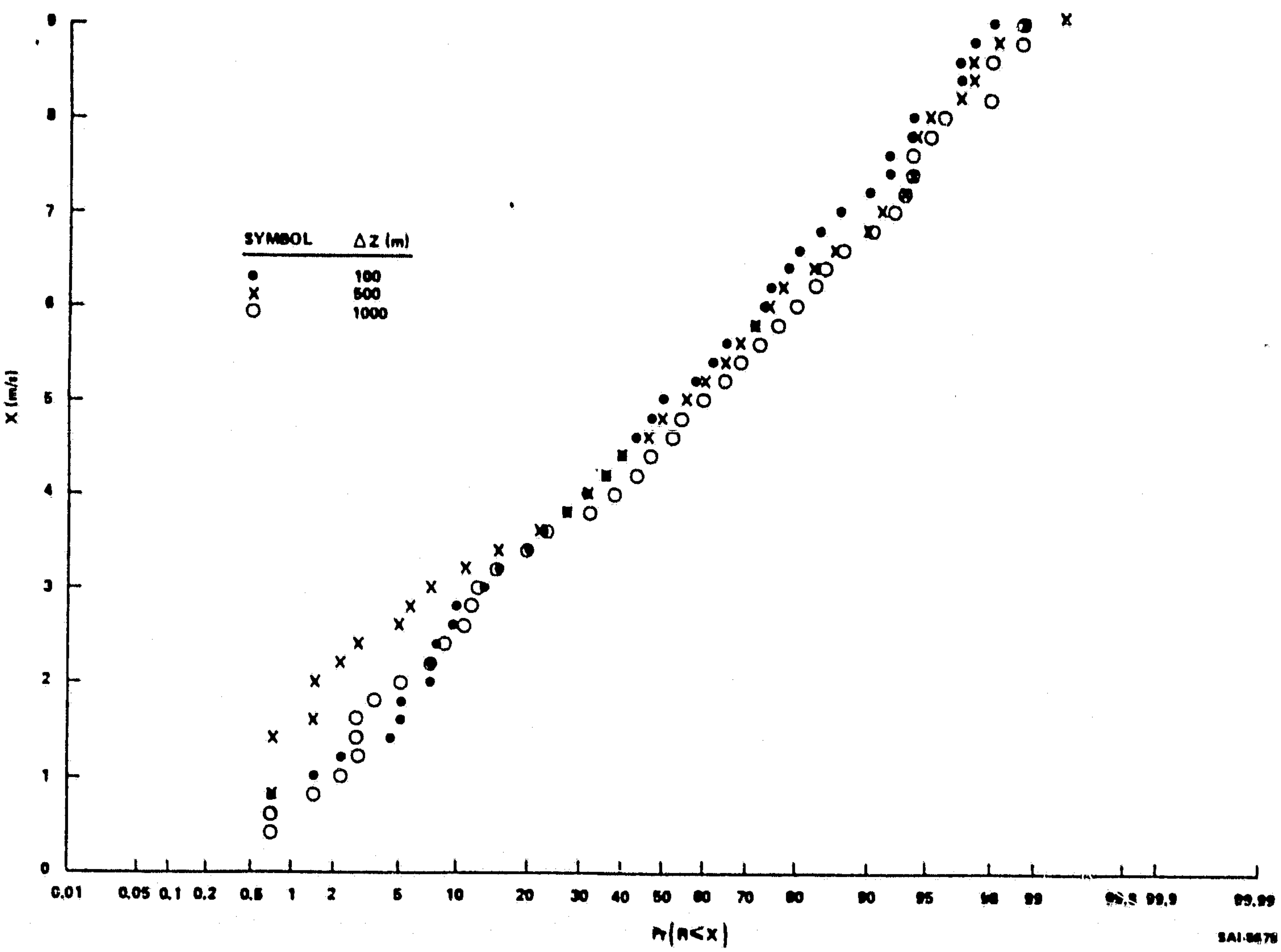

Figure 25. Observed Distribution of Gust (90<λ<2,470m) Modulus, R, Associated with Maximum Wind Shear in Jimsphere Profiles for Layer Thicknesses of 100, 500, and 1,000m During April at Cape Kennedy

It is indicated that the distribution of gust speed associated with maximum wind speed can be accurately fitted with a Gamma distribution. The distributions associated with maximum wind shear are approximately normal; the slight systemmatic upward displacement of the distributions illustrated in Figure 25 supports the conclusion that gusts associated with maximum shear tend to be slightly larger when the layer thickness is small.

A comparison of percentiles of various distributions of gust modulus calculated in this study is presented in Table 8.

TABLE 8. COMPARISON OF PERCENTILES FROM VARIOUS DISTRIBUTIONS OF GUST MODULUS CALCULATED FROM TOTAL RESIDUAL PROFILES (90 < λ < 2,470m) DURING APRIL AT CAPE KENNEDY

(m/s)

Distribution	Reference	50	80	90	95	99 Percentile
Maximum	Fig. 13	6.9	8.3	8.9	9.5	10.3
H_o = 14 km	Table 7	4.0	5.5	6.4	7.6	9.2
Associated with R_{max} in Jimsphere profile	Fig. 24	4.3	5.7	6.6	7.5	9.9
Associated with maximum vector shear in Jimsphere profile	Fig. 25					
	ΔZ(m) 100	5.0	6.6	7.3	8.2	8.9
	500	4.9	6.3	6.8	8.0	9.0
	1000	4.6	6.0	6.7	7.8	9.0

D. Component Gusts

Component gusts, as defined in Section IIF, are analyzed here as a function of altitude (6, 8, 10, 12, and 14 km) month (February and April) and filter type.

Percentiles calculated for the observed probability distributions of zonal and meridional gusts are listed in Tables 9 and 10.

Table 9. Observed Percentiles of Zonal Component Gust in High-Pass Filtered[1] Jimsphere Profiles at Cape Kennedy

FEBRUARY (m/s)

ALTITUDE (KM)	DATA	1	5	10	20	50	80	90	95	99	PERCENTILE	N
6	RPII	−3.50*	−2.19	−1.97*	−1.54	0.00	1.49*	1.88	2.27*	2.70*		11
	TRP	−4.10*	−2.74*	−2.31*	−1.90*	−0.48	1.84*	2.32	2.72*	3.30		
8	RPII	−3.25	−2.03*	−2.08	−1.49	0.53	1.48*	1.90*	2.58*	3.55*		10
	TRP	−3.75	−2.97*	−2.40	−1.86	0.40	1.91*	2.47*	3.02*	4.05*		
10	RPII	−3.35*	−2.55*	−2.17*	−1.82*	−0.44	1.66*	2.16*	3.10*	4.15*		16
	TRP	−4.05*	−3.26*	−2.70*	−2.12*	−0.40	2.07*	2.70*	3.30*	4.75*		
12	RPII	−5.30*	−3.30	−2.55	−1.80	0.50	2.58*	4.00*	4.95*	6.37*		10
	TRP	−6.10*	−4.10	−3.15	−2.25	0.00	3.25*	4.60*	5.50*	7.35*		
14	RPII	−5.25	−3.77	−3.20	−2.24	1.25	2.93	3.86	4.30	5.10		0
	TRP	−5.70	−4.70	−4.07	−2.67	0.90	3.50	4.60	5.30	6.30		

APRIL (m/s)

ALTITUDE (KM)	DATA	1	5	10	20	50	80	90	95	99	PERCENTILE	N
6	RPII	−3.10	−2.25*	−1.83	−1.55*	−0.07	1.38	1.83*	2.22	2.50		3
	TRP	−3.75	−2.73	−2.27	−1.83	0.07	1.63	2.32	2.70	3.30		
8	RPII	−3.70*	−2.36	−2.13*	−1.69*	0.05	1.29	1.72	2.14	2.57		6
	TRP	−4.10*	−2.78	−2.52*	−2.05*	0.50	1.62	1.97	2.45	3.05		
10	RPII	−3.10	−2.18	−1.85	−1.40	−0.33	1.16	1.66	1.98	2.50		0
	TRP	−3.96	−2.78	−2.25	−1.60	−0.31	1.49	1.94	2.30	3.10		
12	RPII	−4.18	−3.50*	−2.92*	−2.04*	−0.20	2.37	2.85	3.45	4.50		5
	TRP	−5.30	−4.10	−3.40*	−2.60*	0.30	2.87	3.33	4.03	5.30		
14	RPII	−6.50*	−4.20*	−3.37*	−2.66*	1.53	3.63*	4.27*	5.35*	6.75*		16
	TRP	−7.70*	−4.90*	−4.12	−3.47*	1.60	4.10*	5.00*	6.05*	8.10*		

*LARGER ABSOLUTE VALUE BASED ON COMPARISON BY MONTH

(1) WAVELENGTH RANGE OF FILTERED PROFILES:

RPII 420 – 2,470 m

TRP 90 – 2,470 m

SAI-6707

Table 10. Observed Percentiles of Meridional Component Gust in High-Pass Filtered[1] Jimsphere Profiles at Cape Kennedy

FEBRUARY (m/s)

ALTITUDE (KM)	DATA	1	5	10	20	50	80	90	95	99	PERCENTILE	N
6	RPII	−2.96	−2.58	−2.30*	−1.65*	−0.30	1.70	2.12	2.65	3.70		5
	TRP	−3.77	−3.17*	−2.70*	−2.15*	−0.40	1.94	2.48	3.05	4.30		
8	RPII	−3.35	−2.83*	−2.30*	−1.73*	0.63	1.64*	2.60*	3.05*	3.85*		15
	TRP	−4.10*	−3.30*	−2.73*	−2.03*	−0.15	1.90*	2.80*	3.30*	4.50*		
10	RPII	−4.55*	−3.50*	−2.88*	−2.20*	−0.40	2.08*	2.64*	3.30*	4.90*		16
	TRP	−5.65*	−4.10*	−3.50*	−2.55*	0.00	2.37*	3.10*	3.75*	5.70*		
12	RPII	−6.05	−4.78*	−3.70	−2.40	0.60	2.68*	3.56*	4.45*	5.35*		12
	TRP	−7.35*	−5.90*	−4.70*	−3.00	0.73	3.70*	4.50*	5.30*	6.50*		
14	RPII	−8.10*	−4.70	−3.90	−3.17	−1.00	2.80	3.60	4.90	6.10*		5
	TRP	−10.1*	−5.95	−5.25	−4.05	−0.16	3.53	5.00*	5.90*	7.75		
APRIL (m/s)												
6	RPII	−3.50*	−2.63*	−2.20	−1.60	0.30	1.83*	2.16*	3.30*	4.45*		11
	TRP	−4.05*	−3.10	−2.57	−1.88	−0.20	2.20*	2.66*	3.35*	4.50*		
8	RPII	−3.55*	−2.63	−2.15	−1.58	−0.20	1.55	2.12	2.67	3.17		1
	TRP	−3.50	−3.03	−2.45	−1.85	0.17	1.83	2.55	2.96	3.95		
10	RPII	−3.30	−2.65	−2.25	−1.73	0.25	1.67	2.20	2.52	3.70		0
	TRP	−4.10	−3.18	−2.73	−2.00	−0.20	1.48	2.63	3.10	4.70		
12	RPII	−6.10	−4.55	−3.80*	−2.67*	−0.50	1.93	3.13	3.54	3.78		4
	TRP	−7.30	−5.70	−4.40	−3.20*	0.20	2.70	4.15	4.36	4.72		
14	RPII	−7.70	−5.56*	−4.91*	−3.95*	−1.00	3.00*	3.80*	4.90	5.85		10
	TRP	−8.50	−6.77*	−6.00*	−4.80*	−0.20	3.67*	4.70	5.75	8.30*		

*LARGER ABSOLUTE VALUE BASED ON COMPARISON BY MONTH

(1) WAVELENGTH RANGE OF FILTERED PROFILES

RPII	420 – 2,470 m
TRP	90 – 2,470 m

SAI-[illegible]

The distributions were calculated from RP II profiles ($420 < \lambda < 2,470m$) and TRP profiles ($90 < \lambda < 2,470m$). The difference between the percentiles for the two types of filtered profiles is attributable to gust in the wavelength range from 90 to 420 m. These differences rarely exceed 1.5 m/s; the largest difference noted in the tabular data is 2.0 m/s at the 1.0 percentile of the meridional component during February. These differences can increase somewhat at extreme percentiles (<1, >99) not given in the tables. As indicated in Table 11, the largest observed extremal in the 90 to 420m wavelength range at the same reference altitudes is -2.61 m/s (April meridional component at 12 km). In comparison, the largest extremal in RP II and TRP profiles is 9.96 and 11.70 m/s, respectively.

The asterisks in Tables 9 and 10 indicate the larger absolute value based on a February to April comparison for equivalent percentile, altitude and filter type; the 50 percentile was not included in the comparison. The number of percentiles, N, for a particular altitude and month that exceed the corresponding percentiles for the other month is a measure of the relative strength of gusts for the two months. The following criteria were used to evaluate the relative strength of gusts:

N	Relative Strength	Tendency
0, 1, 2, 3	Smaller	Strong
4, 5, 6	Smaller	Moderate
7, 8, 9	Equal	None
10, 11, 12	Larger	Moderate
13, 14, 15, 16	Larger	Strong

February gusts have a moderate to strong tendency to be larger at 6, 8, 10 and 12 km for the zonal component and at 8, 10 and 12 km for the meridional component. April zonal gusts have a strong tendency to be larger at 14 km; April meridional gusts have a moderate tendency to be larger at 6 and 14 km.

The probability distributions of the gust components are "S" shaped and cannot be fitted to a high degree of accuracy with a normal distribution. The probability distributions of the gust components during April at 12 km for RPI ($90 < \lambda < 420m$) profiles (Figure 26) and RP II ($420 < \lambda < 2470m$) profiles (Figure 27) illustrate the "S"

Table 11. Observed Extremal[1] Gust Component in Three Types of High-Pass Filtered Jimsphere Profiles[2] at Cape Kennedy

FEBRUARY (m/s)

ALTITUDE (KM)	RP–I u	RP–I v	RP–II u	RP–II v	TRP u	TRP v
6	– 1,29		– 4,22		– 4.59	
		– 0,91		4.16		4,70
8	1.22		3.87		– 4.38	
		1.36		3.95		4,56
10	1.50		4,73		5.67	
		1,78		6.37		7.82
12	– 1,86		6.70		– 7,75	
		2.25		6.11		– 7,44
14	1,70		7,76		8.67	
		2.07		8.75		– 10.72

APRIL (m/s)

ALTITUDE (KM)	RP–I u	RP–I v	RP–II u	RP–II v	TRP u	TRP v
6	0.97		3.41		4.02	
		– 1,35		4,57		4,57
8	1,86		–4,02		4,53	
		– 1,41		5.59		6.30
10	1.30		–3,02		– 4.00	
		– 1,03		5.06		5.90
12	– 1.68		4.57		– 6.29	
		– 2.61		– 6.56		– 8.08
14	1.85		9.96		11.70	
		2.28		– 8.07		– 9.53

(1) EXTREMAL WITH LARGEST ABSOLUTE VALUE.

(2) WAVELENGTH RANGE OF FILTERED PROFILES:

SAI-5681

RP–I	90 – 420 m
RP–II	420 – 2470
TRP	90 - 2470

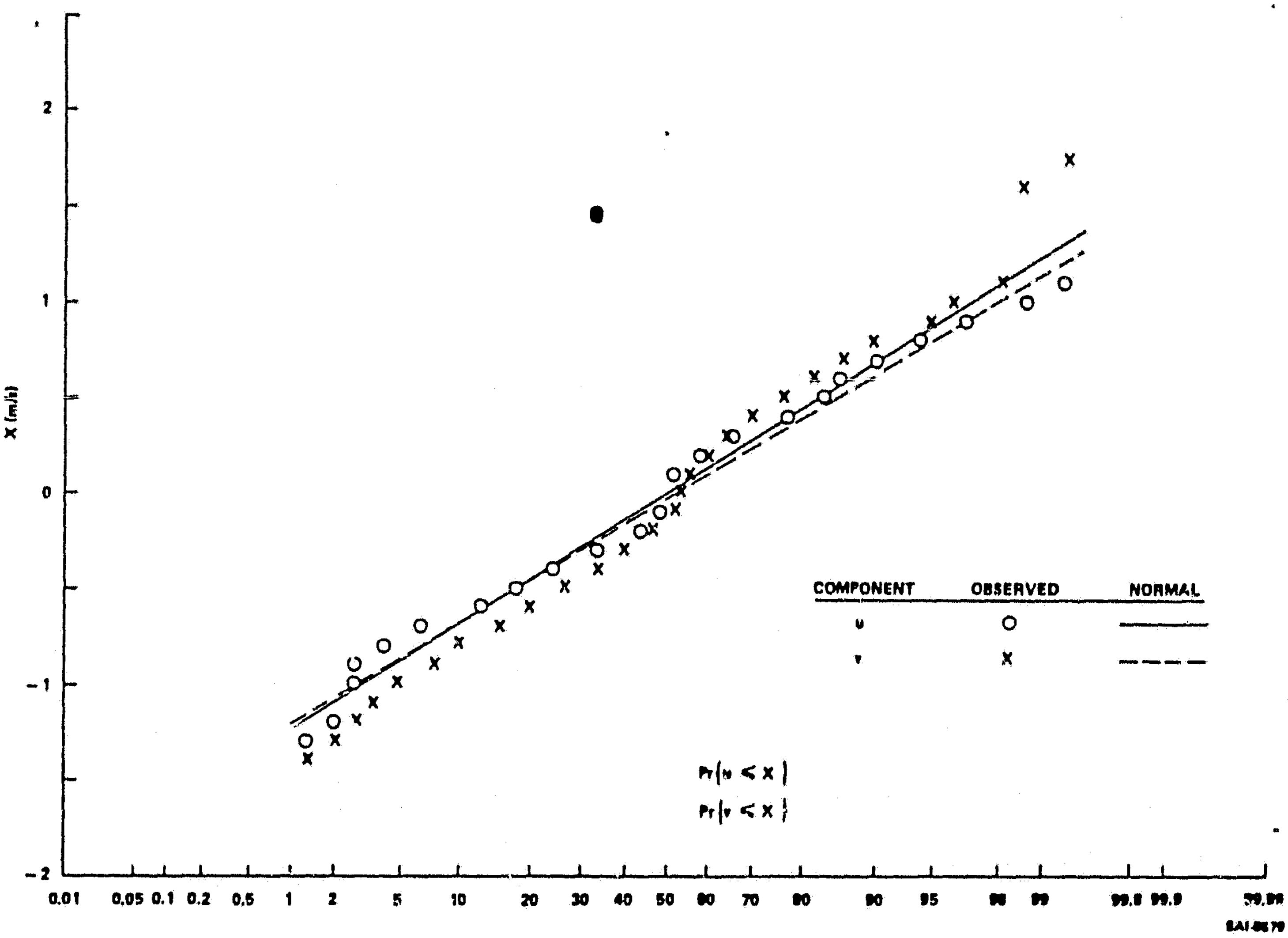

Figure 26. Observed Distribution of Component Gust (90<λ<420m) at 12 km During April at Cape Kennedy (Calculated from Residual I Profiles)

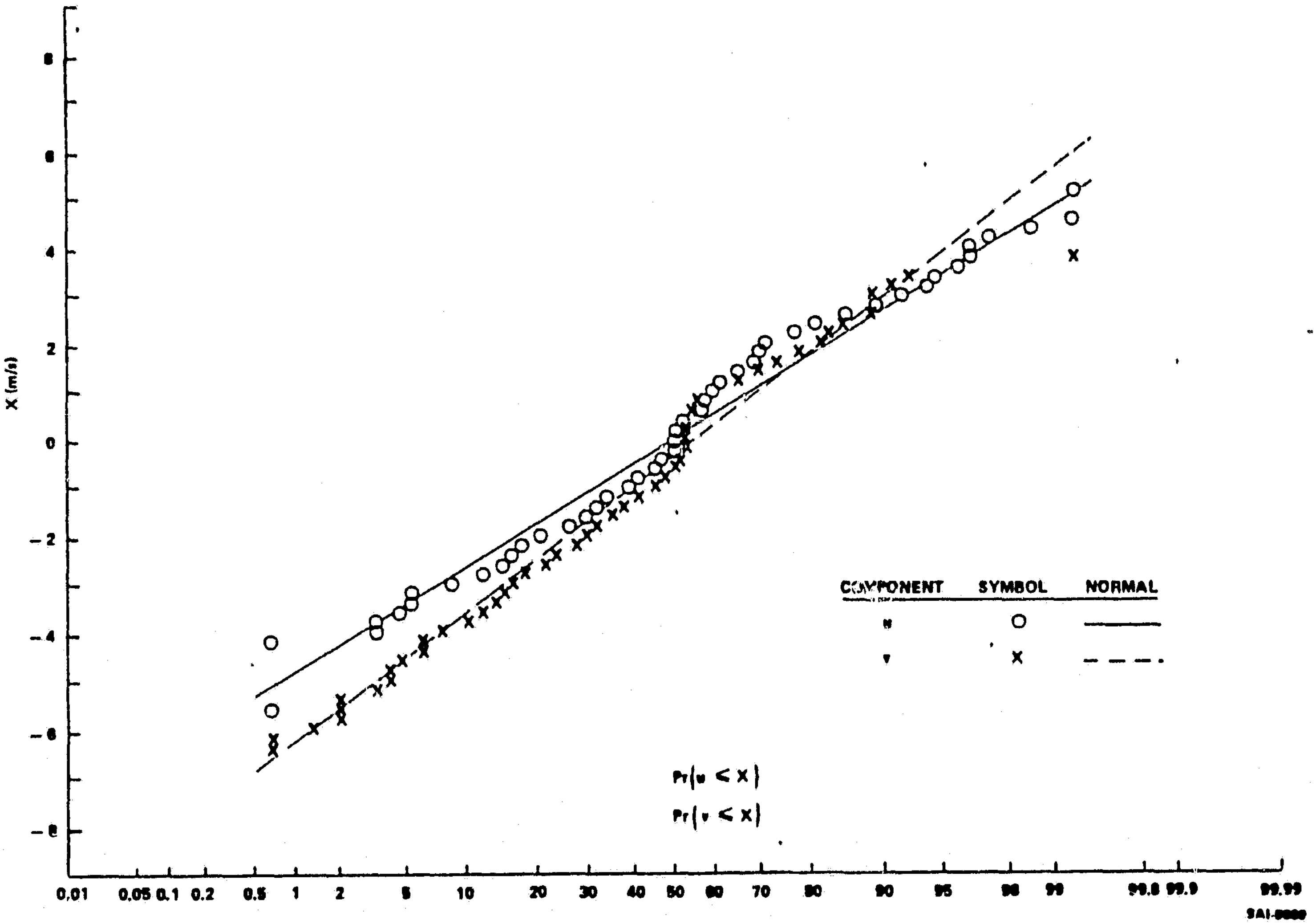

Figure 27. Observed Distribution of Component Gust (420<λ<2,470m) at 12 km During April at Cape Kennedy (Calculated from Residual II Profiles)

shape. Distributions of this type have a probability density function which has two maxima. If the maxima are nearly symmetrical about zero, the density function of the absolute values has a single maximum and the shape of the probability distribution can be accurately approximated by a gamma distribution. The form of the gamma distribution for gust components is the same as Equation 14 (Section III.A) with either $|u|$ or $|v|$ substituted for R_{max}.

An example of the observed and theoretical (gamma) distribution of $|u|$ during February and April at 12 km is illustrated in Figure 28. A list of statistics pertinent to the calculation of theoretical distributions for $|u|$ and $|v|$ for TRP profiles is given in Table 12.

E. Component Gusts Associated with Maximum Wind Speed and Maximum Wind Shear

Component gusts associated with maximum wind speed and maximum vector wind shear in unfiltered Jimsphere profiles were derived from April data according to the procedure outlined below:

- The altitude of maximum wind speed was identified.
- The altitude of the top of the layer containing the maximum vector shear was identified for shear layer thicknesses of 100, 500, and 1,000m.
- The altitudes described above were used for determination of gust component amplitudes in high-pass filtered (TRP) profiles ($90 < \lambda < 2{,}470$) according to the procedure described in Section II.A.6. This yielded four sets of component gust data (three associated with maximum shear and one associated with maximum wind speed).

The distributions of gust components associated with maximum shear are illustrated in Figures 29 (zonal) and 30 (meridional). All the distribution have an "S" shape which is characteristic of a probability density function with two maxima. It is indicated that 70 percent of the zonal component gusts associated with the larger vector wind shears (ΔZ=500 and 1,000m) are negative. Meridional component gusts do not exhibit such a strong bias.

Distributions of gust components associated with maximum wind speed are illustrated in Figure 31. These distributions also exhibit and "S" shape. A large percentage (>94%) of zonal component gusts associated with maximum wind speed are positive; a smaller percentage (61%) of meridional gusts are also biased but in the opposite sense (negative). Therefore, it could be concluded that the contribution of gust in the wavelength range from 90 to 2,470m to the maximum wind speed in a Jimsphere profile is more likely to be positive than negative.

Table 12. Mean, Standard Deviation and Parameters γ and β of the Gamma Distribution for Absolute Component Gust in Total Residual Profiles ($90<\lambda<2,470$m) at Cape Kennedy

FEBRUARY

	6 KM		8 KM		10 KM		12 KM		14 KM	
	$\|u\|$	$\|v\|$	$\|u\|$	$\|v\|$	$\|u\|$	$\|v\|$	$\|u\|$	$\|v\|$	$\|u\|$	$\|v\|$
MEAN (m/s)	1.62	1.86	1.72	1.81	1.90	2.25	2.63	3.07	2.88	3.57
S. D. (m/s)	0.90	0.97	0.94	1.07	1.08	1.33	1.72	1.80	1.58	2.00
β (m/s)	0.50	0.51	0.512	0.63	0.61	0.79	1.13	1.06	0.87	1.12
γ	3.24	3.68	3.35	2.86	3.10	2.86	2.34	2.91	3.31	3.19

APRIL

	6 KM		8 KM		10 KM		12 KM		14 KM	
	$\|u\|$	$\|v\|$	$\|u\|$	$\|v\|$	$\|u\|$	$\|v\|$	$\|u\|$	$\|v\|$	$\|u\|$	$\|v\|$
MEAN (m/s)	1.59	1.87	1.59	1.72	1.45	1.81	2.37	2.73	3.37	3.69
S. D. (m/s)	0.86	1.01	0.84	0.99	0.82	1.10	1.32	1.60	1.90	2.07
β (m/s)	0.47	0.55	0.44	0.57	0.46	0.67	0.74	0.94	1.07	1.16
γ	3.42	3.43	3.58	3.02	3.13	2.71	3.22	2.91	3.15	3.18

SAI-5693

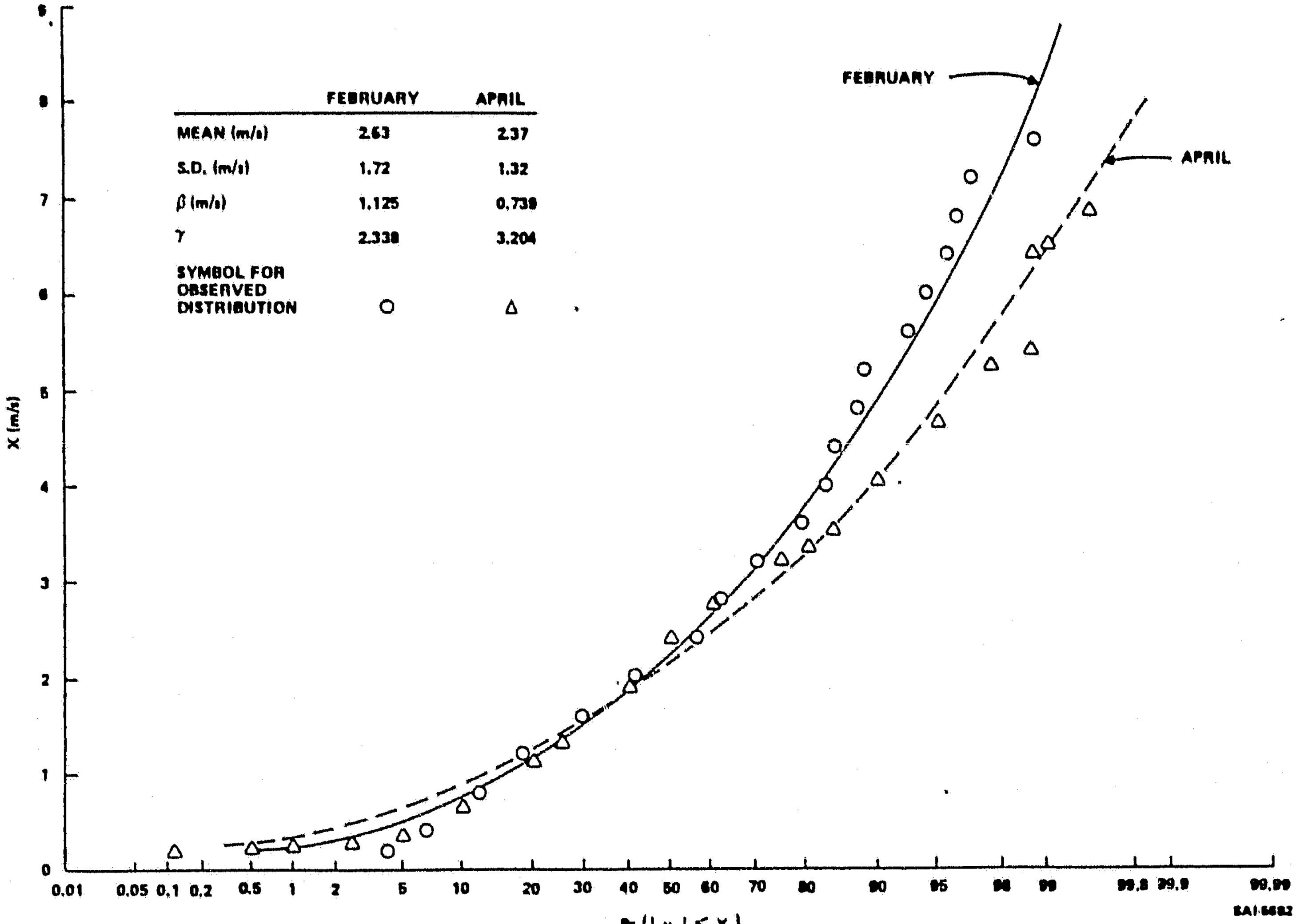

Figure 28. Observed and Theoretical (Gamma) Distribution of Absolute Value of Zonal Component Gust (90<λ<2,470m) at 12 km During February and April at Cape Kennedy

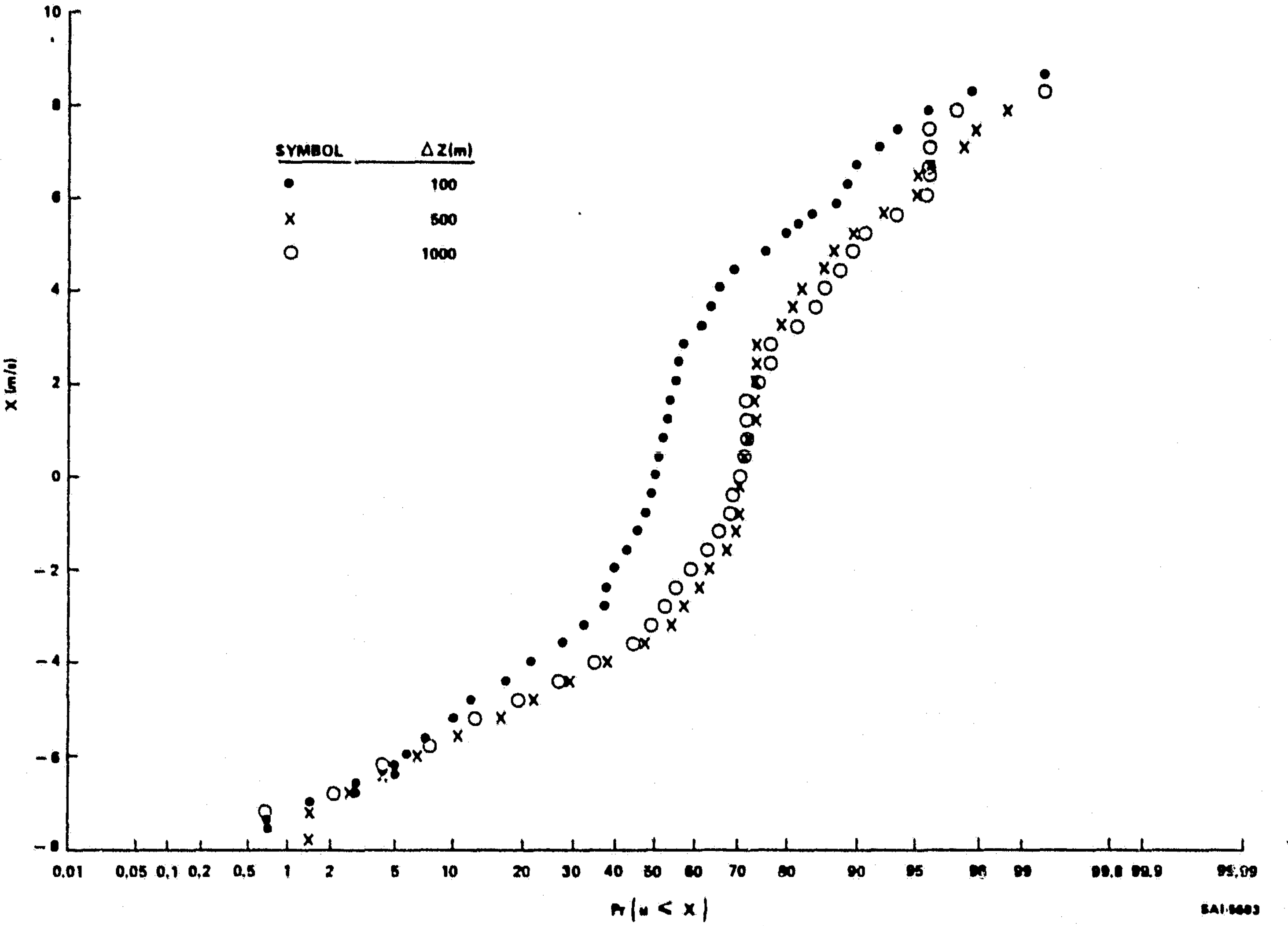

Figure 29. Distribution of Zonal Component Gust (90<λ<2,470m) Associated with Maximum Vector Shear in Jimsphere Profiles for Layer Thicknesses, ΔZ, of 100, 500, and 1,000m During April at Cape Kennedy

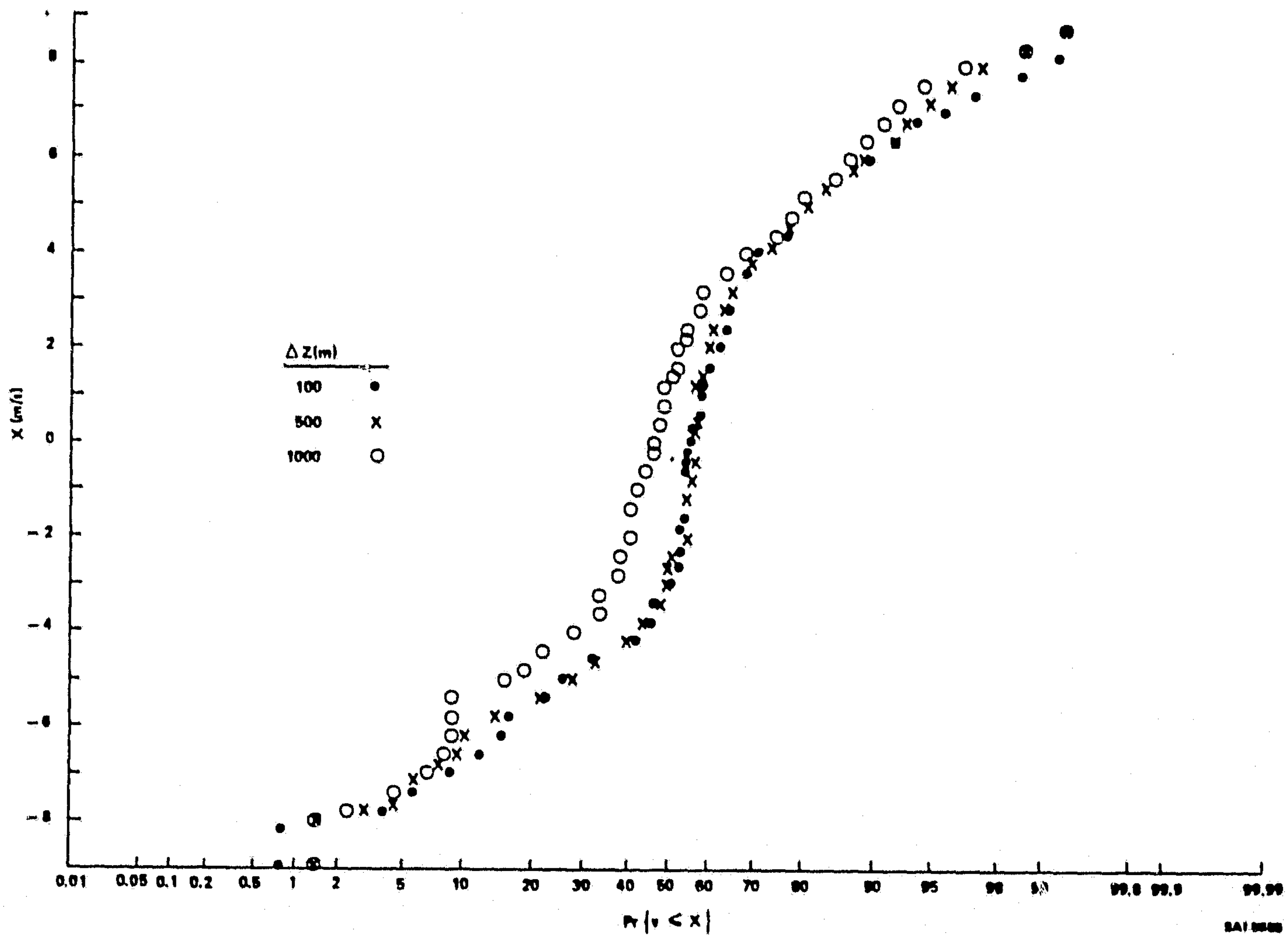

Figure 30. Distribution of Meridional Component Gust (90<λ<2,470m) Associated with Maximum Vector Shear in Jimsphere Profiles for Layer Thicknesses, ΔZ, of 100, 500, and 1,000m During April at Cape Kennedy

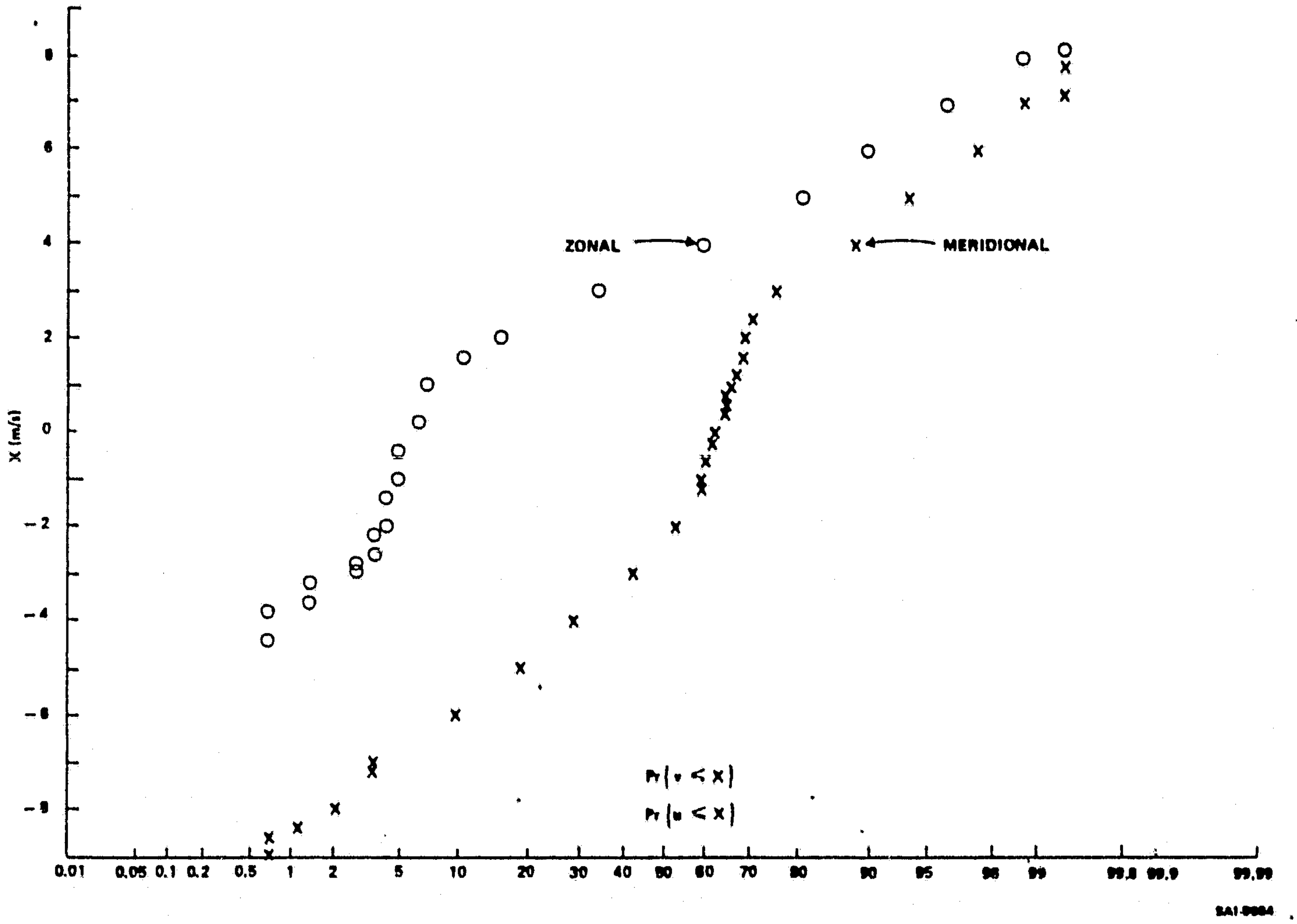

Figure 31. Distribution of Component Gust (90<λ<2,470m) Associated with Maximum Wind Speed in Jimsphere Profiles During April at Cape Kennedy

Extreme percentiles of component gust ($90 < \lambda < 2,470$m) distribution are compared in Table 13. A strong similarity between all but one of the distributions is noted; the exception is the relatively small negative zonal component gusts associated with maximum wind speed. Gusts associated with maximum wind shear or maximum wind speed are not significantly larger than those at a reference height of 14 km.

F. Gust Length

Gust length, L, as defined in Section II.A.5 is analyzed herein as a function of altitude (6, 8, 10, 12, and 14 km) and month February and April) for TRP data ($90 < \lambda < 2,470$m).

Percentiles calculated from the observed probability distributions of L for zonal and meridional component gust are listed in Table 14. It is indicated that there are no significant trends in the percentiles as a function of altitude, month and component. The observed and theoretical (gamma) distribution of L at 12 km is illustrated in Figure 32. The parameters for the gamma distribution illustrated in Figure 32 were calculated from meridional component gust length data at 12 km during April. The gamma distribution can provide an accurate estimate of the observed distribution. The observed distribution is bounded at the large gust length end of the distribution by the filtering process used to derive TRP profiles; therefore, the gamma distribution, which is unbounded at large gust length, is not valid outside the gust length range of the observed distribution. From this it is suggested that a beta distribution may provide a more accurate approximation.

The beta distribution is of the form

$$Pr \left\{ L \leq T \right\} = \frac{(\alpha+\overset{\star}{\beta}+1)!}{\alpha!\overset{\star}{\beta}!} \int_{o}^{T} t^{\alpha}(1-t)^{\overset{\star}{\beta}} dt \qquad (19)$$

$$\text{where } t = x/x_{max} \quad (0 \leq t \leq 1) \qquad (20)$$

The parameters α and $\overset{\star}{\beta}$ are estimated from the sample mean, $\overline{X}$, and standard deviation, σ, according to

$$\alpha = Kb - 1 \qquad (21)$$

$$\overset{\star}{\beta} = b - 1 \qquad (22)$$

Table 13. Observed Extreme Percentiles of Component Gust ($90<\lambda<2,470$m) Distributions During April at Cape Kennedy

u (m/s)

DISTRIBUTION	ΔZ (m)	1	5	10	90	95	99	PERCENTILE
ASSOCIATED WITH MAXIMUM VECTOR SHEAR IN JIMSPHERE PROFILE	100	−7.12	−6.40	−5.21	6.67	7.70	8.36	
	500	−8.06	−6.20	−5.69	5.26	5.99	7.86	
	1000	−7.12	−6.11	−5.41	5.11	5.81	7.97	
ASSOCIATED WITH MAXIMUM WIND SPEED IN JIMSPHERE PROFILE		−3.70	−0.30	1.60	6.10	6.70	8.10	
REFERENCE HEIGHT = 14 KM		−7.70	−4.90	−4.12	5.00	6.05	8.10	

v (m/s)

DISTRIBUTION	ΔZ (m)	1	5	10	90	95	99	PERCENTILE
ASSOCIATED WITH MAXIMUM VECTOR SHEAR IN JIMSPHERE PROFILE	100	−8.17	−7.64	−6.85	6.11	6.96	8.13	
	500	−9.09	−7.38	−6.19	6.19	7.38	8.37	
	1000	−9.09	−7.22	−5.71	6.72	7.71	8.72	
ASSOCIATED WITH MAXIMUM WIND SPEED IN JIMSPHERE PROFILE		−8.50	−6.65	−5.80	4.30	5.55	7.10	
REFERENCE HEIGHT = 14 KM		−8.50	−6.77	−6.00	4.70	5.75	8.30	

SAI-5692

Table 14. Observed Percentiles of Gust Length, L, in TRP ($90<\lambda<2,470m$) Profiles at Cape Kennedy

L (m), APRIL

	6 KM		8 KM		10 KM		12 KM		14 KM	
PERCENTILE	u	v	u	v	u	v	u	v	u	v
1	38	25	55	13	25	19	25	25	15	9
5	90	131	138	125	107	79	88	105	81	42
10	150	188	194	225	141	163	167	180	150	100
20	300	313	350	365	238	309	350	310	360	270
50	609	589	639	694	580	650	625	610	660	556
80	867	856	870	950	950	900	906	875	879	825
90	1025	1027	1088	1213	1117	1017	1067	1075	984	925
95	1142	1144	1235	1363	1275	1175	1159	1213	1131	995
99	1588	1388	1235	1725	1725	1375	1663	1738	1525	1425

L (m), FEBRUARY

	6 KM		8 KM		10 KM		12 KM		14 KM	
PERCENTILE	u	v	u	v	u	v	u	v	u	v
1	54	25	25	10	37	19	13	9	10	10
5	97	135	88	47	96	94	63	42	47	47
10	167	250	134	94	139	170	167	78	117	100
20	317	405	300	317	292	350	250	189	315	263
50	534	659	360	618	613	644	560	593	636	584
80	800	915	880	890	928	960	838	979	959	916
90	1063	1110	1050	1050	1134	1200	1000	1138	1086	1050
95	1213	1215	1275	1175	1225	1413	1257	1263	1231	1155
99	1563	1525	1575	1588	1563	1588	1525	1613	1725	1375

SAI-5896

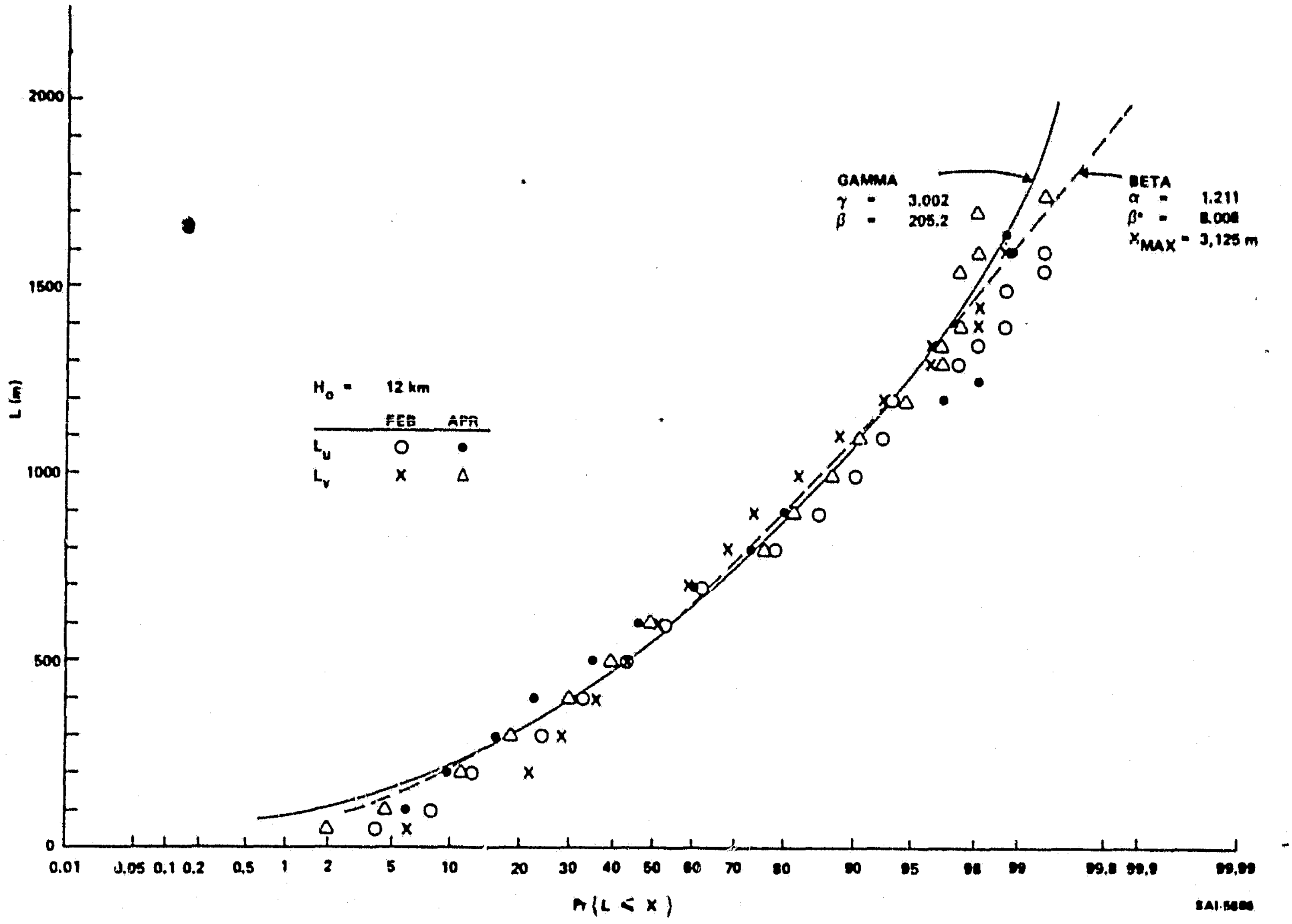

Figure 32. Observed and Theoretical (Gamma and Beta) Distributions of Gust Length Calculated from TRP Profile Data (90<λ<2,470m) at Cape Kennedy

$$K = \frac{\overline{X}/X_{max}}{1-\overline{X}/X_{max}} \tag{23}$$

$$b = \frac{K- (\sigma/X_{max})^2 \ (K+1)^2}{(\sigma/X_{max})^2 \ (K+1)^3} \tag{24}$$

The beta distribution illustrated in Figure 32 was also calculated for the meridional component gust length data at 12 km during April. The value of X_{max} (3,125m) chosen is one-half the wavelength at which the high-pass filter amplitude response for TRP profiles is .10. As illustrated in Figure 32, the beta distribution does not seem to fit the observed distribution with greater accuracy than the gamma distribution.

The parameters of the gamma and beta distributions of gust length are listed in Table 15.

G. Prediction of Monthly Wind Statistics

The year-to-year variability of monthly winds aloft statistics at Cape Kennedy has been documented in a previous study (Ref. 8). The bivariate normal statistics during April at Cape Kennedy during 1958 and 1967 listed below illustrate the magnitude of the variability.

	$\overline{u}$ (m/s)	σ_u (m/s)	$\overline{v}$ (m/s)	σ_v (m/s)	R(u,v)
1958	45.89	19.78	-6.21	16.70	.0176
1967	14.14	12.75	-9.38	7.90	-.1610

For the purpose of launch planning, it is desirable to optimize the selection of monthly wind statistics so that conditions associated with a particular launch are more accurately represented. The selection could be based on 30-day forecasts of synoptic weather patterns issued by NOAA.

An examination of the synoptic patterns during 1958 and 1967 indicates that there is a correlation with certain wind statistics. As indicated in Table 16, the persistant high-pressure ridge over the southeastern U.S. during 1967 resulted in unusually warm and dry conditions; in contrast the synoptic pattern during 1958 favored above normal precipitation and near normal temperature. The rank of each variable during the fifteen-year period (1956-70) is included in the table; for example, the average precipitation of .08 inches in 1967, the smallest in the 15-year period (1956-70), has a rank of 15. The data in the table indicate that the wind statistics are positively correlated with temperature; the correlation with precipitation seems to be higher.

Table 15. Parameters of Theoretical Distributions (Gamma and Beta) of Gust Length at Cape Kennedy

FEBRUARY

		6 (KM)		8 (KM)		10 (KM)		12 (KM)		14 (KM)	
DISTRIBUTION	PARAMETER	L_u	L_v	L_u	L_v	L_u	L_v	L_u	L_v	L_u	L_v
GAMMA	γ	3.30	4.28	2.82	3.23	3.03	3.13	2.92	2.36	2.97	2.83
GAMMA	β (m)	175.65	155.71	210.58	191.59	210.76	217.05	197.31	257.13	215.24	207.42
BETA$^{(1)}$	α	1.50	2.16	1.09	1.40	1.21	1.23	1.20	0.71	1.16	1.11
BETA$^{(1)}$	β^*	9.99	10.63	7.93	8.68	7.59	7.03	8.72	6.08	7.39	8.12

APRIL

		L_u	L_v	L_u	L_v	L_u	L_v	L_u	L_v	L_u	L_u
GAMMA	γ	3.09	3.72	3.74	3.44	2.47	3.46	3.77	3.00	3.77	3.04
GAMMA	β (m)	197.67	163.28	170.87	200.45	248.45	180.57	168.39	205.20	169.45	182.94
BETA$^{(1)}$	α	1.29	1.80	1.77	1.46	0.79	1.57	1.80	1.21	1.79	1.32
BETA$^{(1)}$	β^*	8.43	10.62	9.78	7.68	6.31	9.27	9.98	8.01	9.88	9.72

SAI-5687

(1) FOR X_{MAX} = 3125 m

Table 16. Synoptic Patterns, Wind, Temperature and Precipitation Statistics for April 1958 and 1967. The Rank of Each Statistic for the 15-Year Period [1956-70] is Given within the Brackets

	1958	1967
Magnitude of mean wind vector at 12 km(1) (m/s)	46.3 [1]	17.0 [15]
Total wind variability at 12 km(2) (m/s)	25.9 [1]	15.0 [15]
Synoptic Pattern(3)	Transition from low to high zonal index	Persistent ridge over SE U.S.
Precipitation (in)(4)	3.72 [3]	.08 [15]
Mean Temperature (^{o}f)	70.9 [9]	73.4 [1]

(1) $M = \sqrt{\bar{u}^2 + \bar{v}^2}$

(2) $\sigma = \sqrt{\sigma_u^2 + \sigma_v^2}$

(3) From analyses by R. A. Green, "The Weather and Circulation of April 1967," pp.491-496, Mon. Wea. Rev. Vol 95, N.7 July 1967 and P. Stark, "The Weather and Circulation of April 1958," pp. 132-140, Mon. Wea. Rev. Vol. 86 No. 4, April 1958.

(4) Monthly Average for N. Central Florida Climatic Division

The foregoing examination is the basis for an attempt to predict total wind variability during a future 30-day period at Cape Kennedy given the standard NOAA 30-day forecast (updated every 15 days) of temperature and rainfall. The method is based on the hypothesis that total wind variability at Cape Kennedy is correlated with mean temperature and rainfall over a climatic division (area) near Cape Kennedy. The total wind variability, σ_T, is defined by

$$\sigma_T = \sqrt{\sigma_u^2 + \sigma_v^2} \qquad (25)$$

where, σ_u and σ_v are the standard deviations of the zonal and meridional wind components during a monthly reference period.

The standard NOAA 30-day forecasts of temperature and percipitation are of a qualitative nature and cover large areas. Precipitation predictions are in three broad categories (light, moderate and heavy) each representing one-third of the monthly values that have been observed in the past; similarly, there are five categories (much below, below, near normal, above and much above) for temperature; one-eighth of the observed temperatures that fall in each of the much above and much below normal categories, one-quarter in each of the above and below normal, and near normal categories. The class limits have been determined by NOAA for each month and station from available uniform records. The class limits for Orlando, Florida, during April are given below along with values that have been chosen to represent each category.

Average Temperature ($\overline{T}$)	Class Limits (^{o}F)	Representative Values (^{o}F)
Much Above	$73.4 < \overline{T}$	73.4
Above	$71.9 < T \leq 73.4$	72.7
Near Normal	$70.5 < T \leq 71.9$	71.2
Below	$69.0 < T \leq 70.5$	69.7
Much Below	$T \leq 69.0$	69.0

Precipitation (P)	Class Limits (in)	Representative Values (in)
Heavy	4.18 P	4.18
Moderate	1.52 $P \leq 4.18$	2.85
Light	$P \leq 1.52$	.76

The total wind variability, σ, is estimated by substitution of the representative values of $\overline{T}$ and P into the relation

$$\sigma = 78.68 + 1.50P - .88\overline{T} \qquad (26)$$

The coefficient of multiple correlation between σ, P and $\overline{T}$ is .80. Equation (26) was calculated by the least squares method from data for the period 1956-70; Cape Kennedy wind data and mean values of P and $\overline{T}$ obtained for the North Central Climatic Division of Florida were used.

The correlation between the observed and calculated σ at 12 km during April utilizing $\overline{P}$ and $\overline{T}$ observed during the period 1956 thru 1970 is illustrated in Figure 33. It is shown that even if $\overline{P}$ and $\overline{T}$ are known, or predicted exactly, significant differences exist between the calculated and observed wind variability. These results illustrate the best that can be achieved with this technique. Since the NOAA 30-day forecasts of $\overline{P}$ and $\overline{T}$ are not perfect, a further degradation of the correlation between observed and predicted σ is expected when the forecasted values of $\overline{P}$ and $\overline{T}$ are used in Equation (26); this is illustrated in Figure 34. It is evident from these results that the NOAA 30-day forecast is not sufficiently accurate to be utilized in Equation (26) for the prediction of σ on a long term basis.

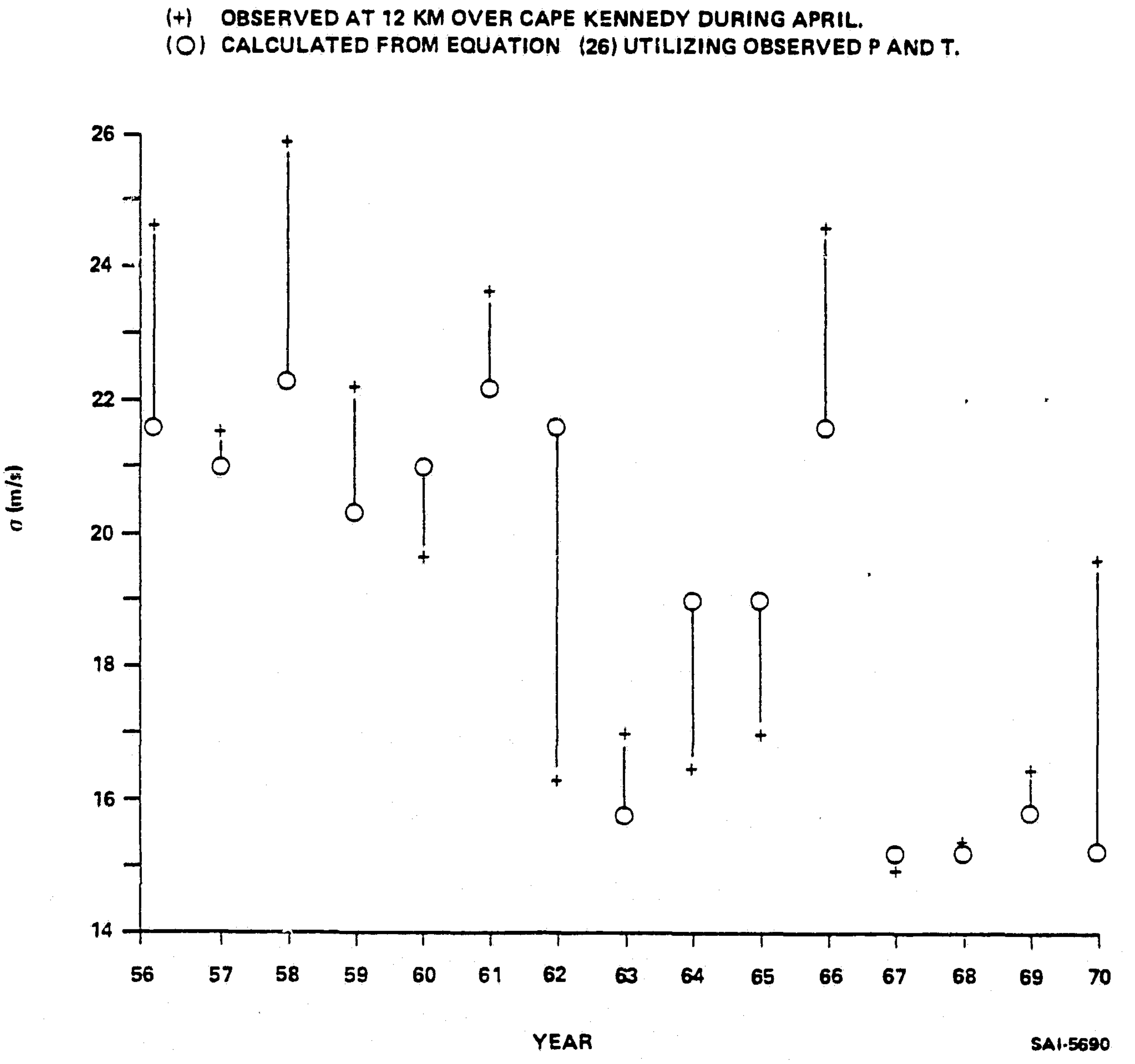

Figure 33. Observed and Calculated σ at 12 km During April at Cape Kennedy Based on Observed $\overline{P}$ and $\overline{T}$

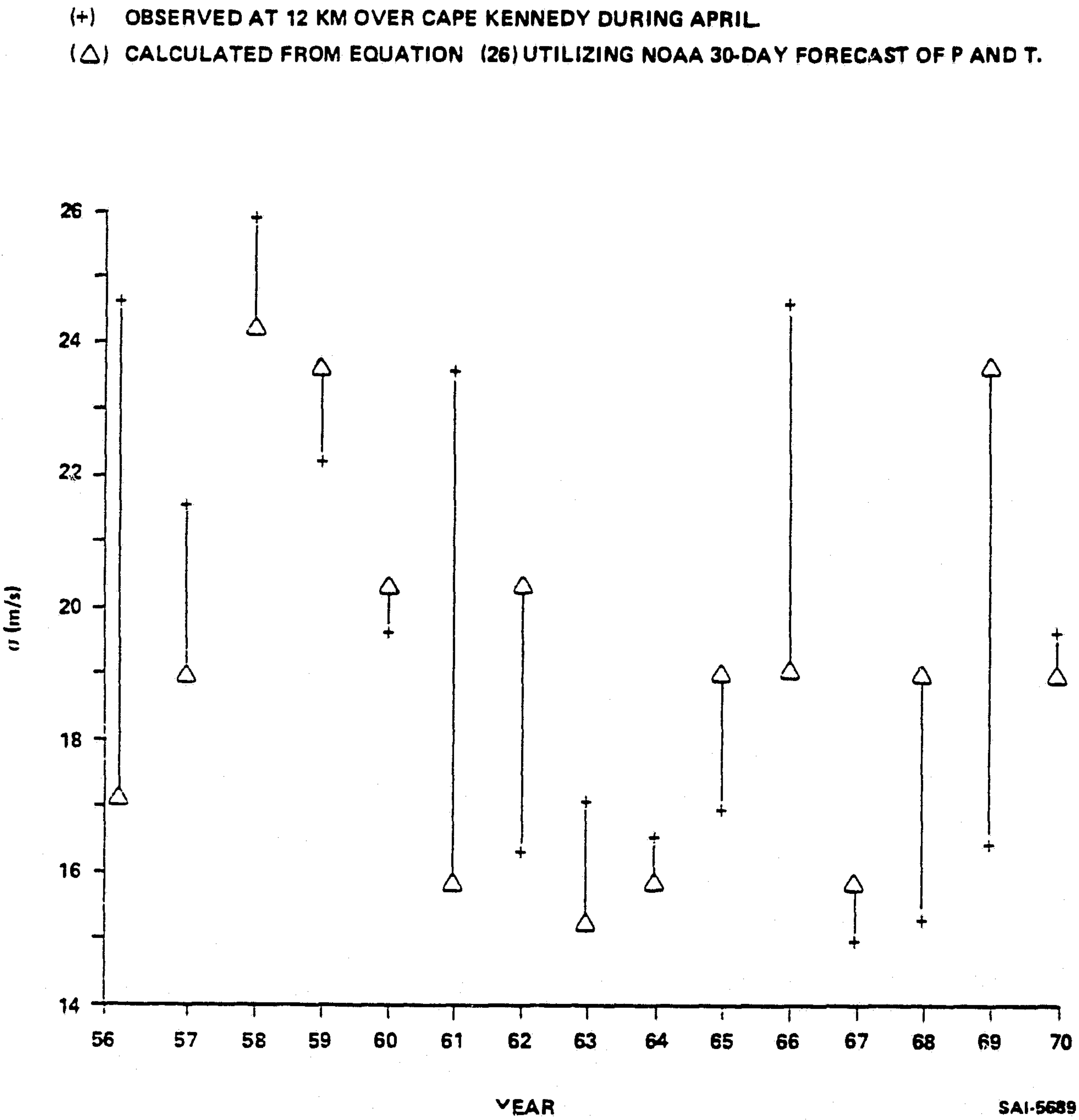

Figure 34. Observed and Calculated σ at 12 km During April at Cape Kennedy Based on NOAA 30-Day Forecast of P and $\overline{T}$

IV. CONCLUSIONS AND RECOMMENDATIONS

Probability distributions of a number of characteristics of detailed wind profiles measured at Cape Kennedy, Florida, have been shown to be accurately represented by a gamma distribution. These characteristics include:

- Maximum vector modulus of filtered and unfiltered Jimsphere wind profiles
- Gust vector modulus at a reference height
- Gust vector modulus associated with maximum wind speed in the unfiltered Jimsphere profile
- Zonal and meridional component gust at a reference height
- Gust length

There is an apparent inconsistency in the conclusions concerning component gust and gust vector modulus at a reference height. If the component gusts are bivariate gamma, then the gust vector modulus would not be univariate gamma as indicated here. Lacking a complete knowledge of the probability distribution of the modulus of a bivariate gamma distributed vector, it can only be concluded that the univariate gamma is a good approximation of that distribution for this data set. The validity of the univariate approximation may be proven if a better understanding of the bivariate gamma distribution and the required simplying assumptions can be developed. It is recommended that methods for calculating the probability distribution of the modulus of the bivariate gamma distributuon be devised.

The results of the study provide a basis for the further development of idealized models for use in flight simulations. These idealized models by themselves cannot represent real wind profiles which have a significant random component. It is recommended that a model consisting of the attributes of both idealized and random gust models be developed.

V. REFERENCES

1. Fichtl, G. H. and Perlmutter, M.: Stochastic Simulation of Vertically Nonhomogeneous Gusts. AIAA Paper 76-389; AIAA Ninth Fluid and Plasma Dynamics Conference, San Diego, California, July, 1976.

2. Kaufman, J. W. (Editor): Terrestrial Environment (Climatic) Criteria Guidelines for Use in Aerospace Vehicle Development, 1977 Revision.

3. Adelfang, S. I. and Court, A.: Jimsphere Wind and Turbulence Exceeding Statistics. NASA CR-2118, NASA, Washington, D. C., August, 1972.

4. Brown, S.C.: 150 per Month Jimsphere Wind Speed Profiles for Aerospace Vehicle Design Capability Studies, KSC, Florida. NASA Document NASA/MSFC-ES81, February, 1978.

5. DeMandel, R.E. and Krivo, S.J.: Study to Improve the Accuracy and Resolution of FPS-16 Radar/Jimsphere Wind Measurements. Lockheed Missiles and Space Company Final Report under NASA Contract NAS8-26128, HREC-6128-2 LMSC-HREC D225068, June 1971.

6. Luers, J., and Engler, N.: On Optimum Methods for Obtaining Wind Data from Balloon Sensors, Journal of Applied Methodology, Vol. 6, No. 5, October 1967, pp. 816-823.

7. DeMandel, R.E. and Krivo, S. J.: Selecting Digital Filters for Application to Detailed Wind Profiles, NASA CR-61325, 1971.

8. Adelfang, S.I.: Analysis of Vector Wind Change with Respect to Time for Vandenberg Air Force Base, Californ[illegible]. NASA CR-159776, August, 1978.

ACKNOWLEDGMENTS

The author acknowledges the outstanding efforts of his coworkers at SAI. Their patience, diligence and competence are strongly reflected in this report. Mr. Willie Robinson was responsible for the computer programming effort, Ms. Ann Jaynes, Ms. Deborah Newby and Mr. William Rhodes prepared this document for publication.

The author expresses his appreciation to his colleague Mr. O. E. Smith of the Aerospace Environment Division, Space Sciences Laboratory for his stimulating discussions, technical review and encouragement.